

# The Neoproterozoic West-Congo “Schisto-Calcaire” sedimentary succession from the Bas-Congo region (Democratic Republic of the Congo) in the frame of regional tentative correlations

Jacques L.H. CAILTEUX<sup>1,\*</sup>, Franck R.A. DELPOMDOR<sup>2</sup>, Jean-Paul NGOIE NDOBANI<sup>1</sup>

<sup>1</sup> Groupe Forrest International (Lubumbashi, DRC), Av. Pasteur, 9, B-1300 Wavre, Belgium. E-mail: jcailteux.geol@gmail.com

\* corresponding author

<sup>2</sup> Department of Earth and Environmental Sciences, Université Libre de Bruxelles, Brussels, Belgium; presently at: CPMTC-GEOLOGIA-IGC-UFMG, Universidade Federal de Minas Gerais, Belo Horizonte, Brazil. E-mail: delpomdor.franck@gmail.com

**ABSTRACT.** New detailed lithological, sedimentological, major chemical,  $\delta^{13}\text{C}$  and  $\delta^{18}\text{O}$  stable isotopes data were obtained from exploration drilling samples on carbonate formations of the Neoproterozoic Schisto-Calcaire Subgroup (> 635-575 Ma) in the Lukala area (Bas-Congo, Democratic Republic of the Congo). This work characterizes and reinterprets the stratigraphical succession from the C2 (Bulu) up to the C4 (Lukunga) formations. The C3 (Luanza) Formation is subdivided into four submembers and the transition of the C3 Formation with both the C2 and C4 formations is examined. New  $\delta^{13}\text{C}$  and  $\delta^{18}\text{O}$  stable isotope data obtained complete the dataset for the Schisto-Calcaire Subgroup in the frame of a correlation with the same succession in Gabon and the Republic of the Congo. The aged equivalent stratigraphic units and lithologies of the West-Congolian (WCB), Katangan (CAC) and Bambuí (SFB) successions are examined, compared and coupled with the available carbon and oxygen isotope values, and a regional correlation is proposed.

**KEYWORDS:** carbonate, major element geochemistry, carbon and oxygen isotopes, lithostratigraphy, chemostratigraphy

## 1. Introduction

The West-Congolian succession is part of the Neoproterozoic Pan-African-Brasiliano orogenic belts that include two N-S-trending orogens, one on the western side (the West Congo Belt from Gabon to Angola, continued by the Kaoko, Gariep and Saldania Belts), and the other on the eastern side (the Mozambique Belt), linked by a third transcontinental orogen comprising the Damara, Central Africa and Zambezi Belts (Fig. 1).

deposits (e.g. Bamba-Kilenda) are known in the West Congo Belt (WCB) of the Democratic Republic of the Congo (DRC).

The West Congolian carbonate series in the DRC are fully recognized for their cement potential, but the palaeoenvironmental conditions are still unclear or not well known for these carbonates, which record a global warming related to the Snowball Earth Hypothesis occurring in extreme greenhouse conditions just after the Marinoan event (Kirschvink, 1992; Hoffman et al., 1998; Hoffman & Schrag, 2002).

In Central Africa, recent data (Delpomdor et al., in revision) concerning syn- and post-Marinoan carbonate sedimentary rocks indicated that these deposits mark a tectonically active deepening-upward cycle recording a regression. It is followed by: (1) a strong carbonate decrease and the change from carbonate to clastic system in deeper basins with the deposition of condensed red claystones or marls, and diamicrites interpreted as debris flows, (2) high-density doloturbidites, and (3) sea-level rise illustrated by lower-density calciturbidites. The overlying carbonates, i.e. the C3 or Luanza Formation, mark the switch from siliciclastic or clastic carbonate to pure carbonate sedimentation due to an excess of production across the carbonate ramp (Delpomdor et al., 2015), facilitating the development of shallow-water subtidal to supratidal depocentres with the development of bioherm reefs (Trompette & Boudzoumou, 1988; Bertrand-Sarfati & Milandou, 1989; Alvarez & Maurin, 1991) and oolitic shoals (Alvarez, 1992, 1995).

This paper is part of a suite of working studies focussed on the palaeoenvironmental conditions of the Neoproterozoic West Congolian carbonate sequences in the DRC. Recent exploration drilling in the Lukala area conducted by the “Cimenterie de Lukala” (CILU, 2009-2012) provided important new fresh material from the top of the lower part of the C3 or Luanza Formation up to the base of the C4 or Lukunga Formation, and gave the opportunity for updating their lithological, sedimentological, chemical and isotopic data. The lithologies of the carbonate sequences are examined and compared with various analyses such as major element geochemistry, C and O stable isotopes, in order to constraint new stratigraphic subdivisions on the basis of the general depositional setting and sedimentary palaeoenvironmental conditions. Moreover, correlations within the Neoproterozoic West Congo Basin successions are examined.

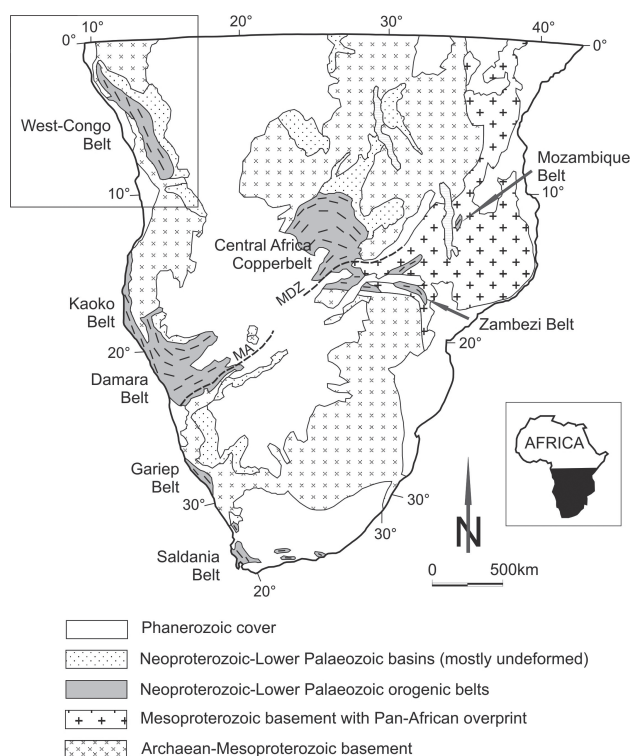


**Figure 1.** Location of the Neoproterozoic orogenic belts and basins in the Precambrian tectonic framework of southern Africa (modified after Hanson, 2003); MA = Matchless Amphibolite; MDZ = Mwembeshi Dislocation Zone.

Contrastingly to the Damara and Central Africa Belts that host numerous well known major polymetallic deposits (stratiform Cu-Co and carbonate-hosted Zn-Pb-Cu-V-Cd-Ag-Ge-Ga; Kampunzu et al., 2009), only few Cu-Pb-Zn occurrences or

## 2. Geological background

The Neoproterozoic WCB stretches N-S over 1400 km long and 150 - 300 km wide along the western margin of the Congo Craton, and extends from southwestern Gabon, crossing the Republic of the Congo (RC) and the DRC, up to northwestern Angola (Fig. 2).

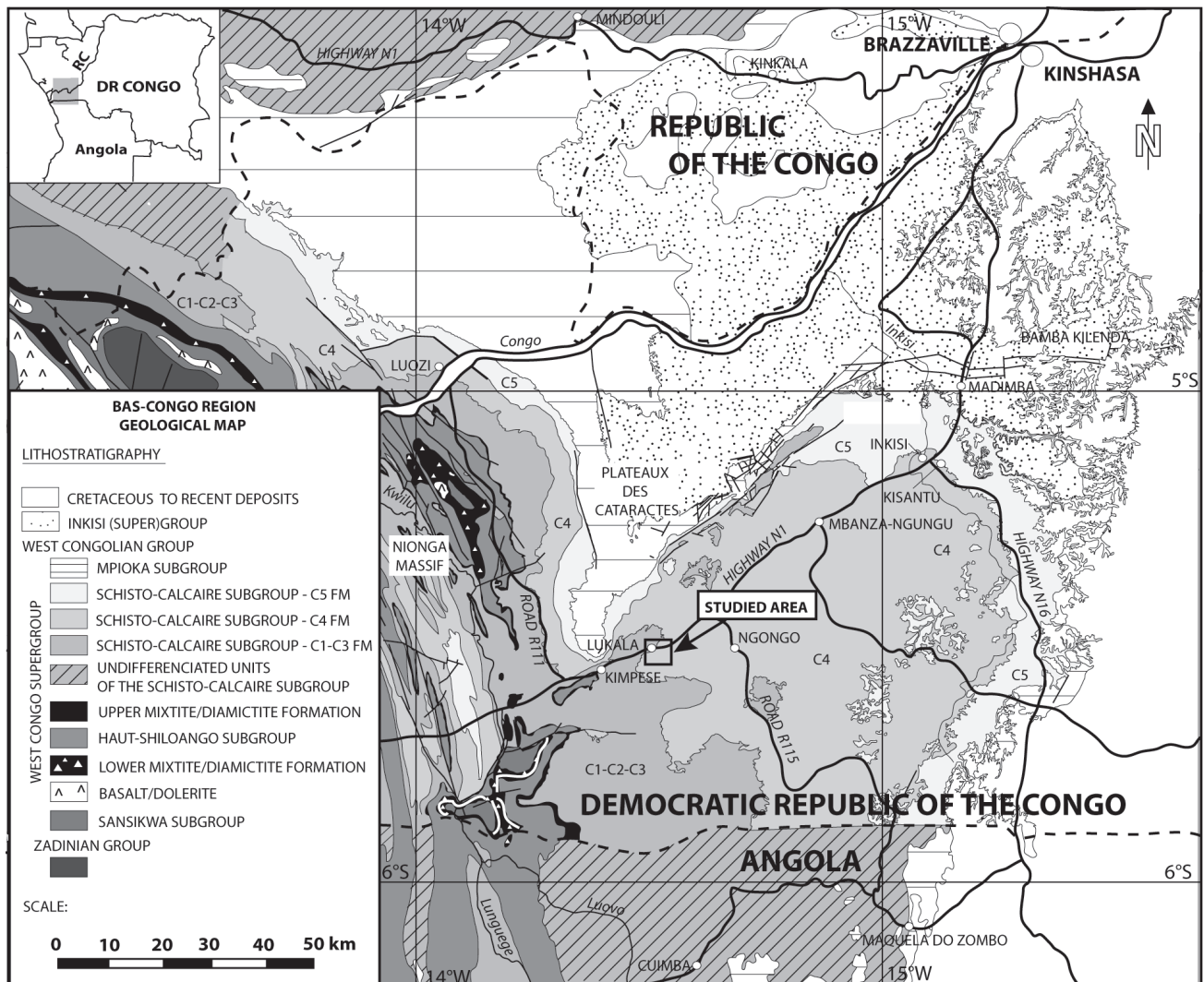


Figure 2. Simplified geological map of the West Congo Belt (modified after Delpomdor et al., in revision).

The WCB is a thrust-fold-belt with thrust direction oriented to the east (Tack et al., 2001), resulting from a continent-continent collision between the active São Francisco (Brazil) margin and the western margin of the Congo craton (Brito-Neves et al. 1999; Cordani et al. 2003) during the western Gondwana amalgamation (870 to 566 Ma; Kröner & Stern, 2005). This orogenic system, represented by the WCB and its Brazilian Araçuaí belt counterpart, is constrained by well documented syn- (ca. 585-560 Ma) to post- (ca. 530-490 Ma) collisional magmatism, with a paroxysm around 580-560 Ma (Pedrosa-Soares et al., 2011).

The WCB is composed of two different tectonic and metamorphic domains: (1) the western hinterland or “external” domain, that consists of Palaeoproterozoic (Kimezian) basement rocks folded and thrust to the east on top of (2) progressively younger, weakly to unmetamorphosed Neoproterozoic foreland or “internal” domain in the east, with decreasing regional metamorphism from amphibolite facies up to unmetamorphosed rocks (Frimmel et al., 2006).

### 3. Lithostratigraphy

The “Ouest Congo” (or West Congo) Supergroup (Table 1) is subdivided into the: (1) metabasalts, metaclastites, metarhyolites succession of the Zadinian Group (ca. 1000 Ma - ca. 920 Ma), (2) volcano-sedimentary sequences of the Mayumbian Group (from  $920 \pm 8$  Ma to  $912 \pm 7$  Ma; Tack et al., 2001), (3) West Congolian Group sedimentary succession (from ca. 912 Ma to ca. 566 Ma), and (4) the Inkisi (Sub)Group that probably is of Palaeozoic age and overlain by the Karoo in Angola (Tack et al., 2001).

Both the Zadinian and Mayumbian groups represent early Neoproterozoic magmatic events marking the initial continental

rifting of the Rodinia supercontinent before its breakup (Tack et al., 2001).

The Neoproterozoic West Congolian Group comprises (Table 1): (1) ca. 4000 m-thick pre-Pan-African orogen passive-margin platform siliciclastic and carbonate sequences composed, from oldest to youngest, of the Sansikwa, Haut-Shiloango, and Schisto-Calcaire subgroups, and (2) ca. 1000 m-thick late- to post-Pan-African orogen foreland deposition of the Mpioka Subgroup. The succession includes two regionally extensive glaciogenic diamictites: (1) the up to 400 m-thick Lower Diamictite Formation” (former “Lower Mixtite”), and (2) the up to 150 m-thick Upper Diamictite Formation (former “Upper Mixtite”), located stratigraphically at the base of the Haut-Shiloango and of the Schisto-Calcaire subgroups, respectively (Cahen, 1954). The Lower Diamictite Formation is correlated to the global Sturtian glaciation event, with possibly two pulses between ca. 750 Ma (Frimmel et al., 1996; Borg et al., 2003) and ca. 713 Ma (Allen et al., 2002). The Upper Diamictite Formation is interpreted of Marinoan glaciation age ( $635 \pm 1.2$  Ma in Namibia according to Hoffmann et al., 2004; Kampunzu et al., 2009). Both Lower and Upper Diamictite formations consist of poorly sorted mud-supported conglomerates with angular and rounded clasts.

#### 3.1. The Sansikwa Subgroup

The lowermost Sansikwa Subgroup (up to 1630 m-thick) unconformably overlies the Zadinian and the Mayumbian groups through a basal clayey or arkosic matrix-supported conglomerate including arkose and siliceous shale beds. It comprises mostly siliciclastic rocks: grained to fine grained quartzites, siliceous shales, psammites, grained quartzites with stromatolitic and oolitic cherty beds, and shale with interbedded calcareous sandstones or alternating shales and quartzites to the top (Cahen,

AGE (Ma)		SPG	GROUP	SUBGROUP	UNIT	FORMATION	LITHOLOGY		Thickness m				
542	Early Palaeozoic	OUEST CONGO SUPERGROUP	INKISI	> 920 m	Upper	-	reddish quartzite and shale			?			
						Luvumu	pinkish to reddish shale, siltstone, fine grained feldspathic quartzite			≥ 300			
						Zongo	purple to reddish quartzitic arkoses			≥ 300			
					Lower	Morozi	pinkish to reddish shale, psammite, fine grained quartzite			20-30			
						Fulu	purple to reddish conglomeratic, quartzitic arkoses			300-400			
						Bidi	arkosic conglomerate with quartz, quartzite, chert, carbonate and shale clasts			≤ 15			
530 - 550	Neoproterozoic		WEST CONGOLIAN	MPIOKA ~ 1000 m	566 ± 42 Ma	<i>Tectonic unconformity (Pan-African orogeny)</i>							
Upper						Liansama	"Plateaux des Cataractes" facies		Mpioka s.s.	"Eastern Inkisi river" facies		300	60
						Kubuzi	red siltstone with feldspathic quartzite beds; occasional shale; basal clayey conglomerate			purple-red to brown fine grained feldspathic quartzite; occasional shale thin beds		250	220
Lower						Vampa	reddish to greenish shales, siltstone, feldspathic quartzites with carbonate sandstone and conglomerate beds or layers		Luvemba	greyish quartzite and feldspathic quartzite, with local interbedded conglomerate		410	90
						Bangu and Niari Conglomerate	conglomerate with limestone & chert clasts, and interbedded red shale		Gidinga	greyish-green carbonate sandstone and shale, with interbedded reddish psammite & feldspathic quartzite		≤ 40	?
							greyish to greenish clayey limestones, sometimes dolomitic, with lenticular intraformational breccia and dark cherty levels, reddish to pinkish limestone beds and red calcareous claystone interbeds, grey-greenish claystones with cherts, and reddish calcareous claystones with very thin greenish clayey limestones and pinkish limestones, evolving to reddish sandy claystones and fine-grained feldspathic quartzites						~ 90
SCHISTO-CALCAIRE ~ 1100 m		Ngandu C <sub>IV</sub>			Ngandu	ca.550 Ma							
		Bangu C <sub>III</sub>			Bangu	C <sub>5</sub>	magnesian ± organic limestone and dolomite, with oolite, chert, shale and calcareous shale beds; calcareous conglomerates or breccias at the base, overlain by talceous/silicified oolite or pseudo-oolite lenticular beds in shale ("Kisantu oolite" unit)				155-265		
		Lukunga C <sub>II</sub>			Lukunga	C <sub>4</sub>	clayey limestone or dolomite and stromatolitic or oolitic limestone, with many chert layers or nodules; shale, calcareous shale, psammite and sandstone				~ 300		
		Kwilu C <sub>I</sub>			Luanza	C <sub>3</sub>	ca.575 Ma	massive stromatolitic, oolitic or brecciated limestone with thin layers of greenish shale, bedded limestone or shaly limestone alternating with greenish-grey shale layers				~ 240	
Bulu					C <sub>2</sub>		alternating calcareous shale and sandstone, clayey and sandy limestone, shale				≥ 400		
635							C <sub>1</sub>		pink or grey dolomite; interbedded purple shale layers at top		0-15		
650							Upper Diamictite (former 'Mixtite') Formation		diamictites, mixtites		≤ 150		
710		Cryogenian			HAUT-SHILOANGO ≤ 1050 m	SANSIKWA ≤ 1630 m	694 ± 4 Ma	S <sub>1</sub>	Sh <sub>8</sub>	dark-grey clayey nodular limestone, stromatolitic limestone, limestone breccia at top			
									Sh <sub>7</sub>	dark-grey siliceous shale with clayey limestone nodules; banded calcareous siliceous shale			
									Sh <sub>6</sub>	greyish-green siliceous shale		200-350	
									Sh <sub>5</sub>	whitish to brownish grained feldspathic quartzites			
									Sh <sub>3</sub> - Sh <sub>4</sub>	reddish siliceous shale, banded dolomitic shale and clayey dolomite			
	Sh <sub>2</sub>		greenish to greyish siliceous frequently calcareous shale, with interbedded calcareous sandstone and finely bedded limestone						500-700				
750						Sh <sub>1</sub>	greenish-grey to dark-grey siliceous shales						
850							sandy-calcareous matrix supported conglomerate and quartzite						
						Lower Diamictite (former 'Mixtite') Formation		diamictites, shales, quartzites, (basalts)		≤ 400			
						b	dark shale with interbedded calcareous sandstone ; alternating shale and quartzite		200-250				
1000	Tonian	912 ± 7 Ma	920 Ma	Mayumbian		Zadinian	a	fine grained quartzite, purple psammite and siliceous shale in the lower part; whitish to greyish grained feldspathic quartzite with many interbedded cherts, frequently oolitic or stromatolitic		≤ 875			
							S <sub>1</sub>	purple siliceous shale and psammite, with occasional interbedded purple-grey grained quartzite		≤ 500			
					S <sub>0</sub>		Basal Conglomerate: clayey or arkosic supported conglomerate, with interbedded siliceous shale and arkose		≤ 4.5				
						volcano-plutonic felsic sequence		3000-4000					
						metabasalts, metaclastites		< 1500					
						metarhyolites							
						999 ± 7 Ma Noqui granite							
						Palaeoproterozoic & Archean							

Table 1. Lithostratigraphy of the Ouest Congo Supergroup, geochronological data and ages (according to Cahen, 1954; Lepersonne, 1974; Tack et al., 2001; Kadima et al., 2011).

Subgroup	Unit	Formation	Mber	Sub member	Lithology	thickness m		
SCHISTO-CALCAIRE	CIV	Ngandu (only in the Luozi area)	d		red calcareous shales with very thin green shaly limestones and pink limestones, evolving to red sandy shales and fine-grained feldspathic quartzites	± 90		
			c		grey-greenish shales with cherts			
			b		red to pink limestone beds and red calcareous shale interbeds			
			a		light-grey to green clayey limestones, sometimes dolomitic, with lenticular intraformational breccia and dark cherty levels			
	CIII	C5 Bangu	upper b	upper b2		light-grey dolomitic limestones with oolitic and chert beds to the top	30-50	
				upper b1		black to dark-grey organic dolomites and dolomitic limestones, interbedded with shale and calcareous shales; occurrence of oolitic and chert beds	95-135	
			b		Kisantu oolite: lenticular yellow-green beds of grey to dark-grey silicified oolites or pseudo-oolites interbedded in shales and calcareous shales	10-40		
			a		dolomitic limestones, locally organic; lenticular oolitic beds, calcareous conglomerates and breccias at the base	20-40		
	CII	C4 Lukunga	c			alternating beds of dark greyish shales and sandy to calcareous shales with rare limestone interbeds	± 300	
						lenticular beds of dark-greyish to purple low angle laminated limestones interbedded with greyish to reddish muddy limestones, passing upwards into dark-greyish to pinkish calcitic salt-rich limestones and dolomites with slightly wavy laminar including discrete low-angle or smooth convex-up oblique cross-stratifications, oolitic, stromatolitic and collapse breccia levels		
			a	a2		finely bedded evaporitic dark-red claystones with interbeds of dm-thick yellowish to greyish limestones		> 38
				a1		alternance of greyish clayey-silty dolomitic limestone beds and greenish-grey dolomitic shale beds; ± 2 m-thick evaporitic limestone at the base		7-8
	CI	C3 Luanza	b	b2		± 20 m-thick upper massive oolitic/pisolitic whitish limestones marked by erosional surfaces, stylolitic joints and occasional intra-formational conglomerates, and ± 35 m-thick lower bedded light-grey to whitish limestones; both include ≤ 1 mm-thick greenish-grey shale layers	51-57	
				b1		dominant light-grey bedded limestones with mm- to cm-thick greenish-grey shale layers and rare impure greenish-grey cm- to dm-thick shaly limestone beds	26-45	
			a	a2		dominant light-grey limestone beds with frequent mm- to dm-thick greenish-grey shale layers; locally impure shaly greenish-grey limestone beds	35-43	
				a1		dominant impure shaly greenish-grey limestones alternating with cm- to dm-thick light-grey limestone beds or layers	> 56	
		C2 Bulu	C1 Kwilu	h		greyish to greenish-grey sandy and clayey limestones, with interbedded greyish or greenish shales; greenish calcareous shales with interbedded pinkish nodular limestones	400	
				g		grey limestones with grey-green shale beds		
				f		dark-grey calcareous shales interbedded with grey limestones		
				e		greyish salt-rich limestones with very thin grey-greenish laminated muddy limestone interbeds, passing towards grey-greenish muddy limestones and greyish limestones		
	d				brown limestones at the base; alternating beds of reddish calcareous and sandy shales, passing to grey-greenish muddy limestones interbedded with greyish pure to replaced salt-rich limestones			
	c				alternated red- to rust-coloured calcareous sandstones evolving to reddish calcareous shales and calcareous siltstones			
	b				rust- to purple-coloured calcareous sandstones with planar parallel, convolute and low angle ripple laminations and cross-bedding, interbedded with rust-coloured shales, passing upward to reddish silty shales and pinkish muddy dolomites including mega-scale hummocky cross-bedding; at the top, greyish-green to rust-coloured sandy to calcareous shales with interbeds of sandstones and limestones			
	a				alternated light-grey to white muddy dolostones and rust-coloured silty shales with wavy-lenticular, crossed-ripple, and convolute laminations and low angle climbing ripples			
C1			pinkish or grey low angle dolomites, marked by alternating thin beds of graded light-grey to white muddy dolomites and rust-coloured silty claystones with discrete low-angle or smooth convex-up oblique cross-bedding at the top	0 - 15				

**Table 2.** Lithostratigraphical subdivisions of the Schisto-Calcaire Subgroup (according to Cahen, 1954; Sikorsky, 1958; Lepersonne, 1974; this paper).

1954; Lepersonne, 1974). It is interpreted as a continental rift fill because of its continental crustal basement, basal conglomerate, and the fluvial siliciclastic composition of its upper formation (Frimmel et al., 2006). Igneous events are associated to this succession: basaltic lavas interbedded to the bottom of the Lower Diamictite Formation and feeder dolerite sills and dykes with a tholeiitic affinity intruding both the Lower Diamictite Formation and the Sansikwa Subgroup (Lepersonne, 1974; De Paepe et al., 1975).

### 3.2. The Haut-Shiloango Subgroup

The succeeding predominantly siliciclastic Haut-Shiloango Subgroup (up to 1050 m-thick) is marked by a carbonatic lower sequence that reflects a typical post-Sturtian open marine carbonate platform deposition (Frimmel et al., 2006), and forms two transgression-regression cycles (Cahen, 1954; Lepersonne, 1974). The Bembezi (former “Mouyonzi” or “Petite Bembezi”) Formation (500 to 700 m-thick), in the lower part, consists

from bottom to top of basal sandy-calcareous matrix-supported conglomerates and quartzites, passing to bedded siliceous or dolomitic siliceous shales with calcareous sandstones and finely bedded limestones, and to clayey dolomites at the top. In the upper part, the "Sekelolo" unit (200 to 350 m-thick) comprises: (1) grained feldspathic quartzites passing to siliceous shales, (2) shales with clayey carbonate nodules or banded calcareous siliceous shale, (3) limestone breccias, stromatolitic-like limestones, and nodular clayey limestones at the top.

### 3.3. The Schisto-Calcaire Subgroup

The post-Marinoan carbonate-rich succession of the Schisto-Calcaire Subgroup (ca. 1100 m-thick) is considered as post-glacial cap carbonates conformably overlaying the Upper Diamictite Formation. It deposited on a ramp composed of deep-marine outer ramp to shallow-marine inner ramp with oolitic shoal barrier, stromatolitic bioherms, lagoon- and sabkha-type environments (Cahen, 1954, 1978; Alvarez, 1995; Delpomdor, 2007). It was firstly subdivided into four units, the Kwilu, Lukunga, Bangu and Ngandu (Delhaye & Sluys, 1923; Cahen, 1954; Lepersonne, 1974; Cahen & Lepersonne, 1976), and later into five formations (C1 to C5; Tables 1, 2) by Delhaye & Sluys (1920, 1924a, 1924b, 1929) and Lepersonne (1974). The Ngandu unit occurs only in the Luozi region and its relation to the Schisto-Calcaire Subgroup is unclear.

The  $\pm 650$  m-thick Kwilu (C1) unit is subdivided into three formations (C1, C2 and C3) that consist of: (1) a 0 to 15 m-thick pinkish or grey cap carbonates, formed by alternating dolomite and purplish thin shale beds at the top (C1 or Dolomies Roses Formation), (2)  $\pm 400$  m-thick generally clayey and sandy limestones, calcipelites or sandstones, clayey or sandy pelites (C2 or Bulu Formation), and (3)  $\pm 240$  m-thick cyanobacterial and oolitic limestones at the top (C3 or Luanza Formation).

The Lukunga (CII) unit or C4 Formation,  $\pm 300$  m-thick, is marked by a sudden more clastic deposition at the base including an alternation of shales, calcipelites or sandstones with frequent ripple-marks. Sedimentation evolved to clayey limestones or dolomites, stromatolitic or oolitic limestones, and ended with a new clastic material input marked by the deposition of shales, calcipelites, calcareous sandstones containing abundant chert as beds or nodules.

The Bangu (CIII) unit or C5 Formation, up to  $\pm 265$  m-thick, is characterized by a variably dolomitic and/or organic-rich carbonate succession, with oolite, chert, shale and calcelite beds. It is marked by: (1) oolitic beds, lenticular calcareous conglomerates or breccias at the base, and (2) the 10-40 m-thick Kisantu Oolite unit that occurs in the lower part of the formation and consists of lenticular beds of grey to dark-grey silicified oolites or pseudo-oolites interbedded with shales and calcipelites. The presence of organic matter suggests a regressive episode with deposition in more or less closed lagoonal-type basins, and the lithologies indicate a sedimentation close to the coast, partly in quiet lagoonal or wavy conditions (Cahen, 1954; Alvarez & Maurin, 1991).

The Ngandu (CIV) unit is locally identified in the Luozi area close to the Nionga massif at the border area between the DRC and RC. This unit has been firstly described in the Niari Basin from the RC (Cosson, 1955; Nicolini, 1959). In the DRC, the Ngandu (CIV) unit (90 m-thick) contains, from base to top (Delhaye & Sluys, 1929; Mayor, 1951; Cahen & Lepersonne, 1976): (1) light-greyish to -greenish clayey limestones, sometimes dolomitic, with lenticular intraformational breccia and dark cherty levels, (2) reddish to pinkish limestone beds and red calcareous claystone interbeds, (3) grey-greenish claystones with cherts, and (4) reddish calcareous claystones with very thin greenish clayey limestones and pinkish limestones, evolving to reddish sandy claystones and fine-grained feldspathic quartzites.

### 3.4. The Mpioka Subgroup

The sediments of the Mpioka Subgroup deposited on top of the Schisto-Calcaire Subgroup through an erosional, probably karstic, surface, and represent a siliciclastic proximal marine deposition interrupted by some continental episodes (Cahen,

1954; Lepersonne, 1974). It displays a northern  $\sim 1000$  m-thick "Plateaux des Cataractes" (former Bangu) facies (north of the Mbanza-Ngungu anticline), and a  $\geq 370$  m-thick "Eastern Inkisi River" facies (east of the Inkisi river). Both facies are marked by a basal conglomerate (Bangu and Niari Conglomerate Formation), that occurs locally in the Eastern Inkisi River facies.

The succession comprises: (1) a lower sequence of siltstones and shales with alternating carbonate sandstone, feldspathic quartzite and conglomerate beds (Vampa Formation, Cataracte facies) or carbonate sandstones and shales, psammites, feldspathic quartzites with conglomerate beds (Gidinga and Luvemba formations, Eastern Inkisi River facies), and (2) an upper sequence of feldspathic quartzites and siltstones with occasional shale and conglomerate beds (Kubuzi and Liansama formations vs. Mpioka Formation *sensu stricto*). The Mpioka Subgroup is considered as a late-orogenic molasse-type sequences deposited in foreland basin (Tack et al., 2001; Frimmel et al., 2006).

### 3.5. The Inkisi (Sub)Group

The Inkisi (Sub)Group is a tabular sequence completing the sedimentary pile at the top with a predominant reddish quartzitic-arkosic foreland deposition ( $> 920$  m-thick) that displays two major sedimentary cycles comprising each conglomerate and/or arkosic formations in the lower part, grading up to finely grained quartzites, psammites and shales (Cahen, 1954; Lepersonne, 1974). The uppermost quartzitic to clayey formations are not well known in the western Congo region. The Insiki (Sub)Group was recently considered as an individual lithostratigraphic unit separated from the West Congo Group, being: (1) unrelated to the WCB evolution and (2) a post-orogenic deposition (Tack et al., 2001).

## 4. Age of deposition

The age of deposition of the West Congolian Group (Table 1) is poorly constrained by the lack of geochronological data, i.e. igneous intrusions or volcanic ash deposits, and biostratigraphical fossils. The Sansikwa Subgroup is inferred to be between  $923 \pm 43$  Ma,  $961 \pm 22$  Ma and  $960 \pm 15$  Ma,  $979 \pm 31$  Ma based on youngest detrital zircon age (Frimmel et al., 2006; Straathof, 2011), and  $\geq 750$  Ma based on correlation with the overlying Sturtian age Lower Diamictite Formation and the Kaigas glacial event in southern Namibia. New U-Pb crystallization age of  $694 \pm 4$  Ma is reported on baddeleyite grains from the Sumbi-type dolerite sill intruding both the Sansikwa Subgroup and the Lower Diamictite Formation (Straathof, 2011). In the equivalent time Louila Formation in Gabon, rhyolitic tuffs yielded an U-Pb SHRIMP age of  $713 \pm 49$  Ma (Thiéblemont et al., 2009) consistent with the  $709 \pm 20$  Ma detrital zircon age of the upper clastic unit of the Haut-Shiloango (Frimmel et al., 2006). The Haut-Shiloango is therefore considered to be deposited in a time-interval between  $694 \pm 4$  Ma and the ca. 635 Ma Marinoan age Upper Diamictite Formation (Frimmel et al., 2006; Straathof, 2011; Delpomdor & Pr eat, 2013). This is confirmed by near-primary  $^{87}\text{Sr}/^{86}\text{Sr}$  ratios (0.7068-0.7073) indicating a deposition between 720-645 Ma by comparison with the composite Sr isotope curve (Poidevin, 2007). U-Pb detrital zircon grains from the overlying Upper Diamictite Formation yielded a maximum age of  $707 \pm 23$  Ma (Straathof, 2011) consistent with the Marinoan Ghaub Formation.

Age of the Schisto-Calcaire Subgroup is constrained by strontium isotope ratios for its upper formations in the Bas-Congo region (C3 to C5 formations) that vary from 0.7074 to 0.7084, and thereby suggest deposition between ca. 575 to 550 Ma, consistent with a post Marinoan age (Frimmel et al., 2006; Poidevin, 2007; Delpomdor & Pr eat, 2013).

The Sansikwa/Haut-Shiloango/Schisto-Calcaire folded succession, that is part of the external east-verging fold-and-thrust domain (Fig. 2), is affected by a greenschist facies metamorphism (Tack et al., 2001). The estimated age by Frimmel et al. (2006) of this regional greenschist metamorphism at  $566 \pm 42$  Ma pre-date the unmetamorphosed Mpioka-Insiki sequences deposited unconformably on the folded West Congolian Group succession (Table 1). This is consistent with U-Pb data for the

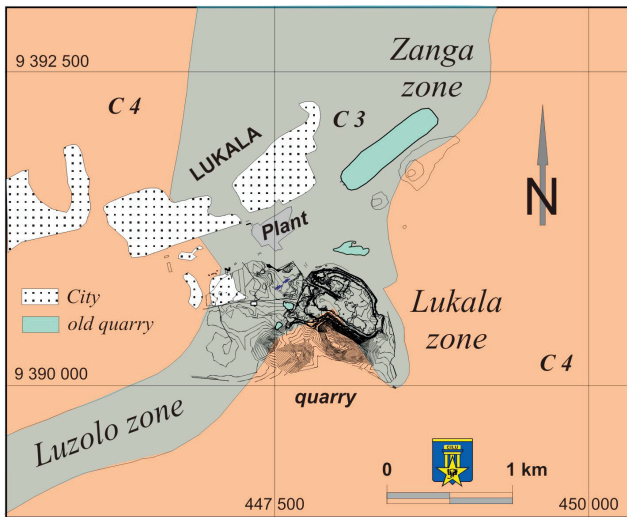


**Figure 3.** Surface geological map in the Lukala area (modified from Dupont, 1972).

Mpioka Subgroup and Inkisi (Sub)Group giving maximum age constraints at  $607 \pm 16$  Ma (Straathof, 2011) and  $558 \pm 29$  Ma (Frimmel et al., 2006), respectively.

Deposition of the tabular post-orogenic Inkisi (Sub)Group at the top of the succession is constrained at best by a maximum age of  $558 \pm 29$  Ma obtained for detrital zircon grains (Frimmel et al., 2006).

## 5. Characterisation of the Schisto-Calcaire Subgroup

### 5.1. Methodology

Detailed lithological logging has been performed on 66 drill cores (totalling 6290 m) from recent exploration by CILU between 2009 and 2012 mainly through the C3 or Luanza Formation. Drill cores cover three exploration zones in the Lukala area: Lukala (s.s., "LUK"), Zanga ("ZAN") and Luzolo ("LZO") (Fig. 3). All the drill holes crossed the C3 Formation and the lower part of the C4 Formation with an excellent core recovery, and were all used in order to reconstruct a reliable local stratigraphy. The fresh core material was sampled generally by 1 metre length (occasionally by 3 metres length). A total of 4172 samples were analysed for CaO, MgO, SiO<sub>2</sub>, Al<sub>2</sub>O<sub>3</sub>, Fe<sub>2</sub>O<sub>3</sub>, loss on ignition (LOI) by the CILU Laboratory in Lukala. In addition, 89 samples collected from the old CICO cores, also drilled through the C3 Formation in the Lukala area and stored at the Royal Museum for Central Africa (Belgium), have been collected for sedimentology, stable isotopic carbon and oxygen (on 19 samples), and major element analysis (on 11 samples). Additional 83 chemical analysis on samples spaced at 50 cm in the first 40 metres of this CICO drill core are presented in this paper (MRAC archives 162 A, 1947).

Carbon and oxygen isotope compositions, that commonly are used for chemostratigraphic correlation of marine carbonate units, were analysed on the different lithological microfacies, selected as homogeneous as possible, from the Lukala core material (from the C3a to C4a members, 18 new samples). Between 1 and 2 mg of powdered whole rock sample has been dissolved with 100% H<sub>3</sub>PO<sub>4</sub> at 75°C in order to extract the CO<sub>2</sub> from the dolomites. The amount of extracted CO<sub>2</sub> at -196°C and its  $\delta^{13}\text{C}_{\text{V-PDB}}$  and  $\delta^{18}\text{O}_{\text{V-PDB}}$

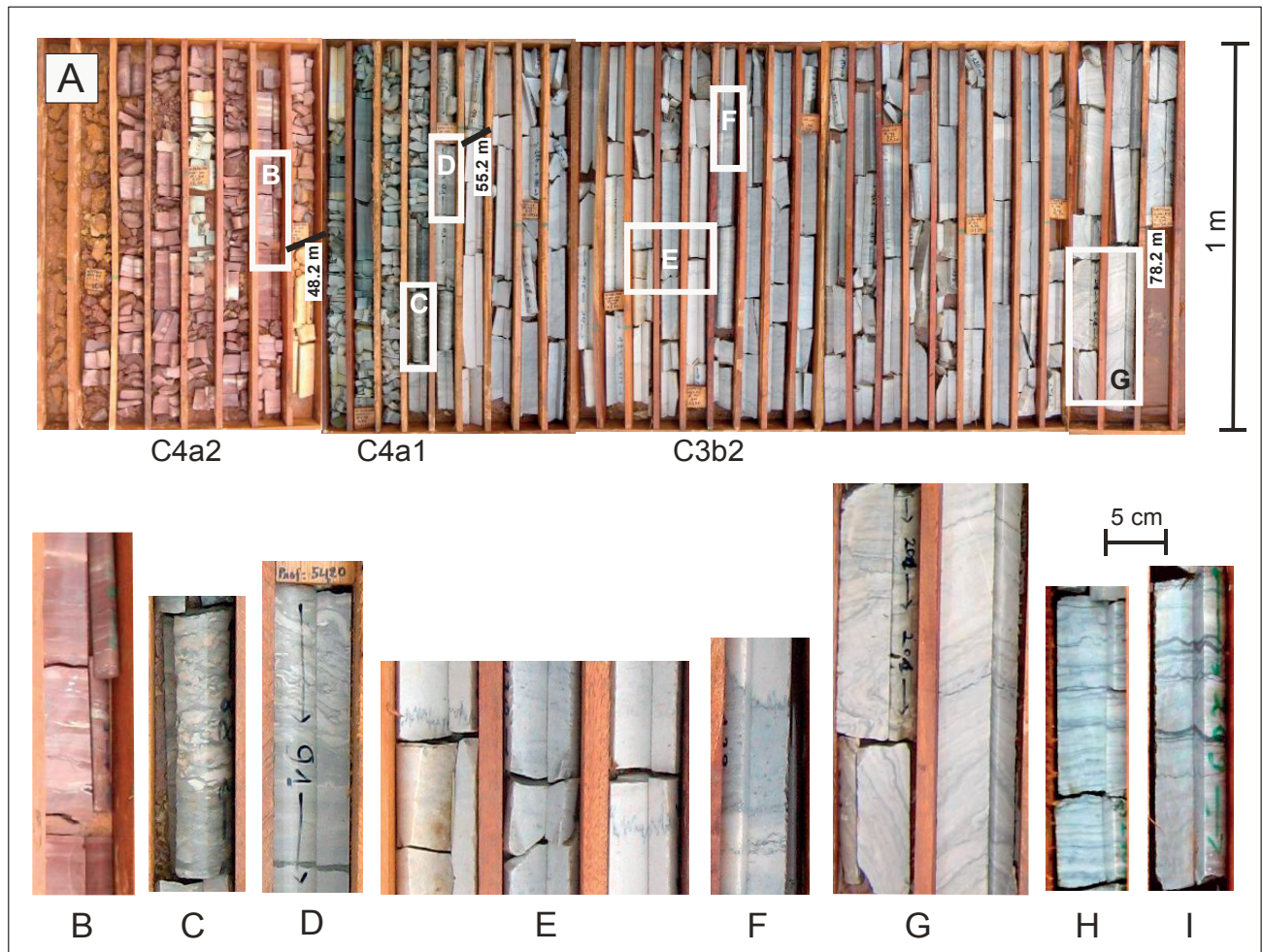


**Figure 4.** (A) Cores of the drill hole LUK-64, C4a2 up to 48.2 m deep (weathered above 42.5 m), C4a1 (48.2-55.2 m), oolitic (55.2-74.9 m) and bedded (74.9-78.2 m) C3b2; (B) core 51/47.2 m, finely bedded evaporitic reddish C4a2 claystones; (C) core 88/53.6 m and (D) core 91/54.2 m: evaporitic greyish C4a1 limestone with collapse breccias; (E) cores 126-136/61-63 m and (F) core 138/63.5 m: C3b2 oolitic limestone with stylolitic joints and erosional surfaces; (G) cores 201/76.2 m - 205/77.7 m, drill hole ZAN-04 (H) core 240/92.5 m and (I) core 269/98.2 m: C3b2 bedded limestone with < 1 mm- to multi mm-thick greenish-grey shale layers.

were measured using a Thermo-Finnigan 252 mass spectrometer at Erlangen University (Germany). The reproducibility of the  $\delta^{13}\text{C}_{\text{V-PDB}}$  and the  $\delta^{18}\text{O}_{\text{V-PDB}}$  measurements is 0.06‰.

## 5.2. New lithological observations

The intersected C3 to C4 formations are described lithologically from youngest to oldest as follows (Table 2).

### 5.2.1. The C4 or Lukunga Formation

This unit includes impure carbonates (limestone, dolostone) and shales, most strongly weathered in the Lukala area. It shows two distinct submembers according to the most complete succession.

a) The C4a2 submember consists of  $\geq 38$  m-thick finely bedded dark red claystones, including (1) centimetric crossbedded sandstone and shale layers forming up to multi-centimetric fining-upward sequences, (2) interbedded decimetric yellowish-white to greyish limestone, and (3) occurrence of pseudomorphs after evaporites in cm-size concentrations (Figs 4A, 4B, 6A).

b) The C4a1 submember contains, from base to top, 6.8 to 7.8 m-thick bedded greyish clayey-silty dolomitic limestones, sometimes calcareous dolomites, with interbedded centimetric to multidecimetric dark- to light-greenish/grey dolomitic shale beds, and evolving to whitish-yellowish evaporitic dolomitic limestones at the top (Figs 4A, 6B). At the base occur  $\pm 2$  m-thick evaporitic grayish to yellowish limestones including calcitic casts or crystals after gypsum collapse breccias (Figs 4A, 4C, 4D). The contact with the underlying C3 Formation is sharp and marked by an erosional surface. A remarkable dissemination or concentration of pyrite occurs in mm- to cm-thick layers near the contact with the C3 Formation.

### 5.2.2. The C3 or Luanza Formation

The C3 or Luanza Formation consists of carbonate rocks subdivided here into 4 submembers (C3b2, C3b1, C3a2, C3a1) according to the importance of a clastic-shaly material that generally decreases from the bottom to the top of the sequence.

This clastic input consists of dark greenish-grey clinocllore associated with illite, of micrometric ( $\mu\text{m}$ ) muscovite, and angular to sub-angular quartz and feldspar silts; it occurs as disseminated grains marking the bedding (Fig. 6E), or forms  $< 1$  mm- up to several mm-thick layers within the carbonate. Minor micron-sized concretions of framboidal pyrite also occur in the clayey layers (Delpomdor, 2007).

a) The C3b2 submember is a high grade limestone unit (95-96%  $\text{CaCO}_3$  in average) that forms the rich body exploited for the cement plant; its thickness reaches 51.2 m to 57.2 m. It is composed from the base to top of: (1)  $\pm 35$  metres whitish to light-grey bedded limestone including some zones with greenish-grey mm- to multi mm-thick shale layers (Figs 4A, 4G, 4H, 4I), overlain by (2)  $\pm 20$  metres whitish to light-grey massive oolitic limestone marked by erosional surfaces, frequent stylolitic joints, occasional intra-formational conglomerates and few  $\leq 1$  mm-thick greenish-grey dolomitic shale layers (Figs 4A, 4E, 4F). The oolitic limestones also contain lumps and rare oncolites (Fig. 6C). Oolites are predominantly spherical or ovoid, and consist of tangential and/or fibro-radial oolites, composite oolites and oolitic aggregates. Vadose pendant beard-like (Dunham, 1971) and/or lamellar microcrystalline calcite cements (Moore & Druckman, 1981; Moore, 1989) are observed around the grains. Millimetric-scale desiccation cracks and pseudomorphs after gypsum and polyhalite (Fig. 6C; Delpomdor et al., 2015) and rare authigenic bipyramidal quartz silts are observed.

b) The C3b1 submember is a  $\pm 26.5$ -45.2 m-thick dominant light-grey bedded limestones with an alternation of: (1) mm- to cm-thick greenish-grey shale layers, and (2) rare cm- to dm-thick greenish-grey impure shaly limestone beds (Fig. 5A). Microbial mats (Fig. 6D) related to *Siphonophycus septatum* are preserved in shale layers (Delpomdor, 2007; Pr eat et al., 2011). The importance of the impure shaly limestone and shale layers highlight two major cycles of variable thickness, both composed of a lower part with dominant more pure limestones followed by a more clayey upper part. Rare dm-thick massive lithoclastic

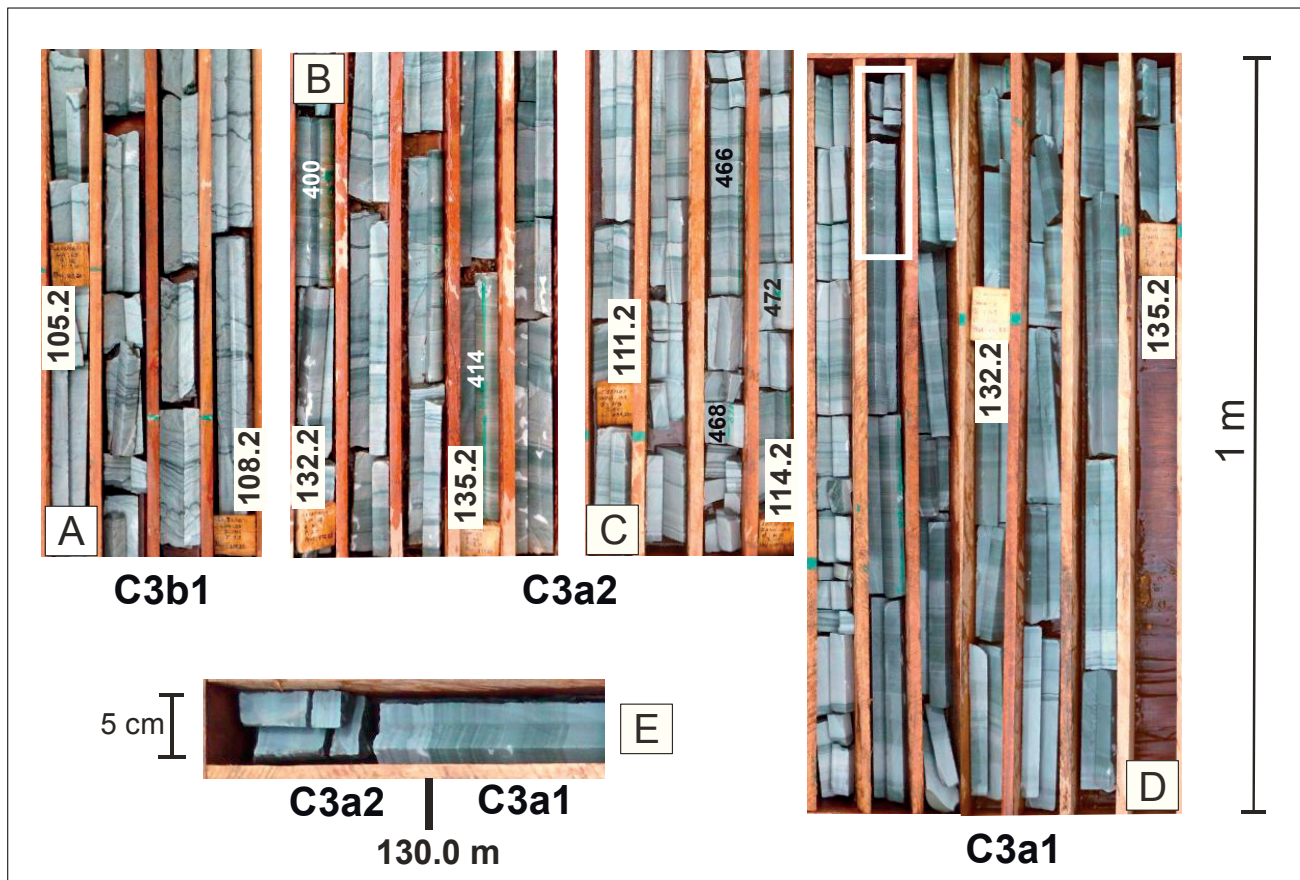


**Figure 5.** (A) Drill hole LUK-69, selected cores between 104.9 and 108.2 m: C3b1 bedded limestone with  $< 1$  mm- to multi mm-thick greenish-grey shale layers; (B) drill hole LUK-69, selected cores between 131.5-136.0 m and (C) drill hole ZAN-11, selected cores between 110.5-114.2: C3a2 bedded limestone with mm- to cm-thick greenish-grey shale layers; (D) drill hole ZAN-11, cores between 129.0-135.2 m: C3a2 in contact with C3a1 impure limestone; (E) cores at the contact between C3a2 and C3a1.

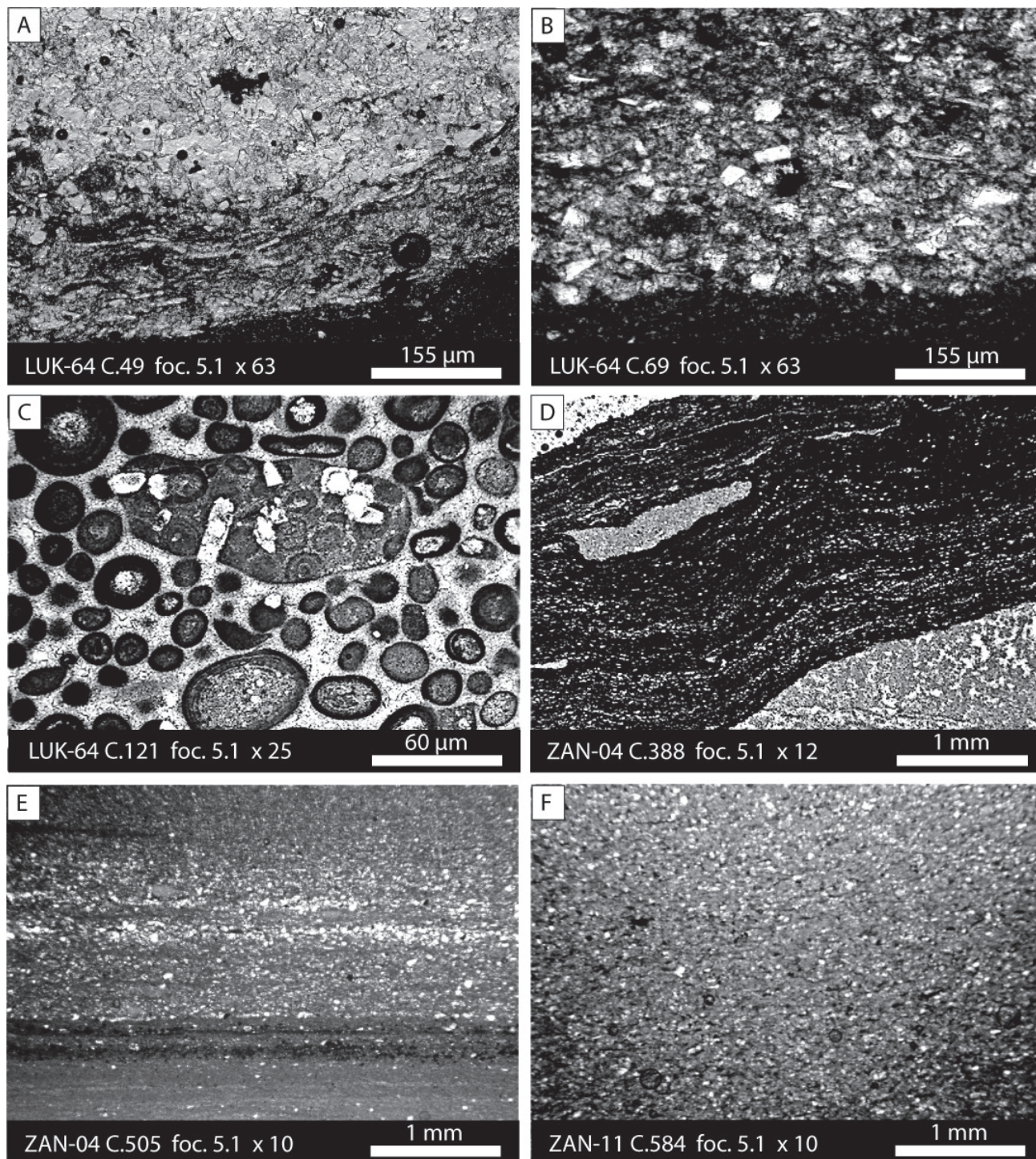


**Figure 6.** Microfacies analysis – (A) micron-thick layers of evaporitic mashes, composed of randomly oriented very fine laths of replaced gypsum, overlying silty limestones, C4a2 submember; (B) Detrital material, including muscovite, quartz and feldspar silts, within laminar dolomitic limestone, C4a1 submember; (C) Oolitic limestone facies with tangential and micritic oolites and lumps in sparry calcite cement. Note the presence of pseudomorphs of evaporites within the nucleus of oolites and inside the lumps, C3b2 submember; (D) Dolomitized cyanobacterial mats in greenish shales, C3b1 submember; (E) Alternation of planar laminated detrital limestones and homogeneous dolomitic limestones; presence of stratified pyrite-rich layers, C3a2 submember; (F) View of detrital limestones, C3a1 submember.

beds contain rounded fragments of dolomitic limestones oriented parallel to stratification.

c) The C3a2 submember shows  $\pm$  35.0-42.6 m-thick dominant light-grey limestone beds, with frequent mm- to multi cm-thick greenish-grey shale layers, and occasional cm- to dm-thick greenish-grey impure shaly limestone beds (Figs 5B, 5C). Under the microscope, this submember displays submillimetric to millimetric planar laminated alternations of fine-grained clayey detrital limestones, including quartz and feldspar silts, micas, clinocllore and illite (Delpomdor, 2007), and homogeneous dolomitic limestones (Fig. 6E).

d) The C3a1 submember was incompletely covered, drilled only on 19 m-thick at Zanga, 49.3 m-thick at Lukala, and 56.2 m-thick at Luzolo. It consists of dominant greenish-grey impure shaly limestone alternating with cm- to dm-thick greyish limestone beds containing frequent cm- to multi-cm-thick greenish-grey shale layers. The contact with the C3a2 submember is clear (Figs 5D, 5E).

No unquestionable lithological marker exists to differentiate the C3a1, C3a2, C3b1 and C3b2 submembers at Lukala. Therefore, it is most convenient to use the fraction of non-carbonate material to differentiate these. The stratigraphic units as defined above

average grades (wt%)	(C) Kwilu 2				Kwilu S	(B) CICO			(A) Lukala area (recent exploration)					
	C2d5	C2d6	C2d7	C2e8	C2e8	C3a2	C3b1	C3b2	C3a1	C3a2	C3b1	C3b2	C4a1	C4a2
CaO	40.28	16.06	36.48	47.68	39.01	33.12	48.38	54.53	34.10	41.20	45.30	52.09	37.34	4.60
MgO	2.72	5.10	3.23	0.72	2.10	3.55	1.07	0.40	3.72	2.69	2.21	1.28	3.14	1.59
SiO <sub>2</sub>	-	-	-	-	-	32.56	13.08	1.45	24.50	16.23	11.62	3.49	21.70	55.56
Al <sub>2</sub> O <sub>3</sub>	0.26	5.23	2.45	0.39	2.09	5.87	2.38	0.85	5.24	3.63	2.62	1.06	4.63	16.21
Fe <sub>2</sub> O <sub>3</sub>	0.77	5.66	2.80	0.80	2.51	2.83	0.85	0.20	2.76	1.86	1.25	0.52	2.20	9.56
SO <sub>3</sub>	-	-	-	-	-	-	0.51	0.37	-	-	-	-	-	-
LOI (wt%)	-	-	-	-	-	-	-	-	27.32	32.66	35.74	40.99	29.68	9.38
CaO : MgO	14.83	3.15	11.28	66.52	18.58	12.47	92.84	162.22	9.16	15.34	20.46	40.75	11.90	2.89
CaO : Al <sub>2</sub> O <sub>3</sub>	152.49	3.07	14.87	123.26	18.63	16.91	30.85	85.65	6.51	11.35	17.30	49.19	8.07	0.28
Al <sub>2</sub> O <sub>3</sub> : SiO <sub>2</sub>	-	-	-	-	-	0.25	0.28	0.63	0.21	0.22	0.23	0.30	0.21	0.29
Ca:Mg max	13.21	2.81	10.05	128.02	16.55	31.57	554.26	547.13	108.64	90.59	208.63	644.32	35.03	20.85
Ca:Mg min	-	-	-	38.45	-	2.75	10.56	25.56	2.92	1.45	4.39	5.70	5.68	0.50
Nber of samples	1	1	1	2	1	9	25	61	142	1135	1678	1164	32	18

**Table 3.** CaO - MgO - SiO<sub>2</sub> - Al<sub>2</sub>O<sub>3</sub> - Fe<sub>2</sub>O<sub>3</sub> - SO<sub>3</sub> - LOI average grades, CaO:MgO, CaO:Al<sub>2</sub>O<sub>3</sub> and Al<sub>2</sub>O<sub>3</sub>:SiO<sub>2</sub> ratios for the C3a1 up to C4a2 submembers of the Schisto-Calcaire Subgroup; (A) samples from the 2009-2012 exploration drilling in the Lukala area (analyses performed by the CILU Laboratory in Lukala); (B) samples from the old CICO drill hole in the Lukala quarry (analyses performed by the CILU Laboratory in Lukala, MRAC archives 162 A, 1947, and Actlabs Canada); (C) samples from the Kwilu 2 and Kwilu S drill holes for the C2d and C2e submembers in the Kwilu area (analyses performed by Actlabs Canada).

are generally recognizable by logging, but locally, especially between the C3a2 and C3b1 submembers, a transition may occur with recurrent beds of more or less pure limestone. In that case, only chemical results (mostly CaO and SiO<sub>2</sub> concentrations) can help in differentiating the submembers

### 5.2.3. The C2 or Bulu Formation

The contact between the C2 and C3 formations has been defined, for the Kwilu area, at the last occurrence of greenish-grey calcareous sandstone beds (Delhaye & Sluys, 1923). Three transitional units comprise from the top to the bottom (Delhaye & Sluys, 1923; Sikorski, 1958): (1) the C2h member (incomplete thickness of ± 29 m) composed of dm-thick beds of green/grey calcareous sandstones with mm- to cm-thick greenish shales, passing to alternations of very thin beds of grey to pink limestones and green shales; (2) the C2g member (19 m in thickness) characterized by cm- to m-thick beds of greyish limestones with grey/green shale layers; and (3) the C2f member (incomplete thickness of ± 15 m) consisting of thin dark-grey calcareous shale beds interbedded within dm- to m-thick grey limestones.

### 5.3. Major element chemistry

Average concentration curves of the recent data set from the Lukala area show an increasing CaO content from the C3a1 submember up to the C3b2 submember, a decrease in the C4a1 submember and a strong depletion in the C4a2 submember. The clastic input (indicated by SiO<sub>2</sub>, Al<sub>2</sub>O<sub>3</sub>, and Fe<sub>2</sub>O<sub>3</sub>) has an opposite evolution (Table 3A, Fig. 7). CaO, SiO<sub>2</sub> and Al<sub>2</sub>O<sub>3</sub> frequency

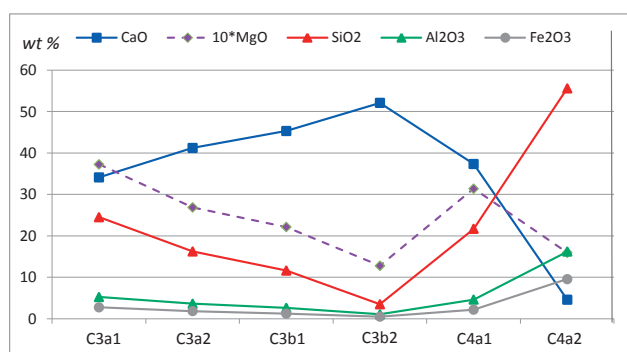


**Figure 7.** Evolution of the CaO - 10\*MgO - SiO<sub>2</sub> - Al<sub>2</sub>O<sub>3</sub> - Fe<sub>2</sub>O<sub>3</sub> average concentrations from the 2009-2012 exploration drilling samples for C3a1 up to C4a2 submembers in the Lukala area.

Gauss curves (Figs 8A, 8B, 8C) show a large distribution of the grades for the C3a1 and the C4a1 submembers, indicating a relative heterogeneity of the sedimentary deposition in terms of clastic input vs. carbonate production. More narrow curves for the

C3a2 and the C3b1 submembers, and narrow curves for the C3b2 submember confirm the progressively more homogeneity of the carbonate deposition. Distribution of the concentrations for the C4a2 submember is very large and completely shifted, reflecting the different nature and a more heterogeneous composition. The MgO Gauss curves (Fig. 8D) show a similar trend as for SiO<sub>2</sub> or as for Al<sub>2</sub>O<sub>3</sub> but with a more narrow distribution in the low content domain (< 5 wt%), except for the C4a2 submember that shows a slightly more dolomitic character. No significant lateral variation of the chemical composition occurs in each unit between the Zanga, Lukala and Luzolo zones of the Lukala area.

Therefore, CaO and Al<sub>2</sub>O<sub>3</sub> concentrations allow differentiation between the C3a1 to the C4a2 submembers. The whole data set of chemical results (n = 4169) shows (Table 3A, Figs 9A, 9B, 9C): (1) a significant input of clastic material during the C3a1 submember, with periods of variable input (average = 5.24 wt% Al<sub>2</sub>O<sub>3</sub>; CaO:Al<sub>2</sub>O<sub>3</sub> = 6.51; n = 142); (2) a global decrease of this clastic input, firstly in the C3a2 submember (average = 3.63 wt% Al<sub>2</sub>O<sub>3</sub>; CaO:Al<sub>2</sub>O<sub>3</sub> = 11.35; n = 1135), and secondly in the C3b1 submember (average = 2.62 wt% Al<sub>2</sub>O<sub>3</sub>; CaO:Al<sub>2</sub>O<sub>3</sub> = 17.30; n = 1678). Both submembers show the same range of values and are composed of cycles with higher followed by lower CaO vs. lower-higher Al<sub>2</sub>O<sub>3</sub> contents; (3) a high purity of the C3b2 limestone (average = 1.06 wt% Al<sub>2</sub>O<sub>3</sub>; CaO:Al<sub>2</sub>O<sub>3</sub> = 49.19; n = 1164), marking a very weak clastic input during this period of deposition; (4) a new episode with the re-occurrence of clastic material in the transitional C4a1 submember (average = 4.63 wt% Al<sub>2</sub>O<sub>3</sub>; CaO:Al<sub>2</sub>O<sub>3</sub> = 8.07; n = 32) and a dominant clastic input in the C4a2 submember (average = 16.21 wt% Al<sub>2</sub>O<sub>3</sub>; CaO:Al<sub>2</sub>O<sub>3</sub> = 0.28; n = 18).

On a CaO vs. Al<sub>2</sub>O<sub>3</sub> graph (Fig. 10A), the C3 formation is aligned on the same trend with increasing CaO and decreasing Al<sub>2</sub>O<sub>3</sub> contents from the C3a1 up to the C3b2 submembers. The C4a1 submember shows a return to less CaO and more Al<sub>2</sub>O<sub>3</sub> contents, while the C4a2 submember appears abruptly depleted in CaO and enriched in Al<sub>2</sub>O<sub>3</sub> contents. On the same graph (Table 3C; Fig. 10A), the C2 or Bulu Formation (C2d, C2e) shows a slightly shifted trend. The CaO:SiO<sub>2</sub> ratios show comparable results as the CaO:Al<sub>2</sub>O<sub>3</sub> ratios, but appear not so accurate owing to the fact that part of the SiO<sub>2</sub> is authigenic (Delpomdor, 2007).

The MgO content in the C3 Formation and in the C4a member is variable and generally follows the inverse trend as for the CaO. Peaks highlight more dolomitic beds (Table 3A; Figs 9A, 9B, 9C). Using the classification of Chilingar (1957, 1960), the Ca:Mg ratios (Tables 3A, 3B; Fig. 10B) highlight that: (1) the C3a1 (Ca:Mg = 2.92 to 108.64; n = 142) and C3a2 (Ca:Mg = 1.45 to 90.59; n = 1144) carbonates vary from dolomites to slightly dolomitic limestones, (2) the C3b1 (Ca:Mg = 4.39 to 554.26; n = 1703) and C3b2 (Ca:Mg = 5.70 to 644.32; n = 1225) carbonates vary from dolomitic to highly calcitic limestones, (3) the C4a1

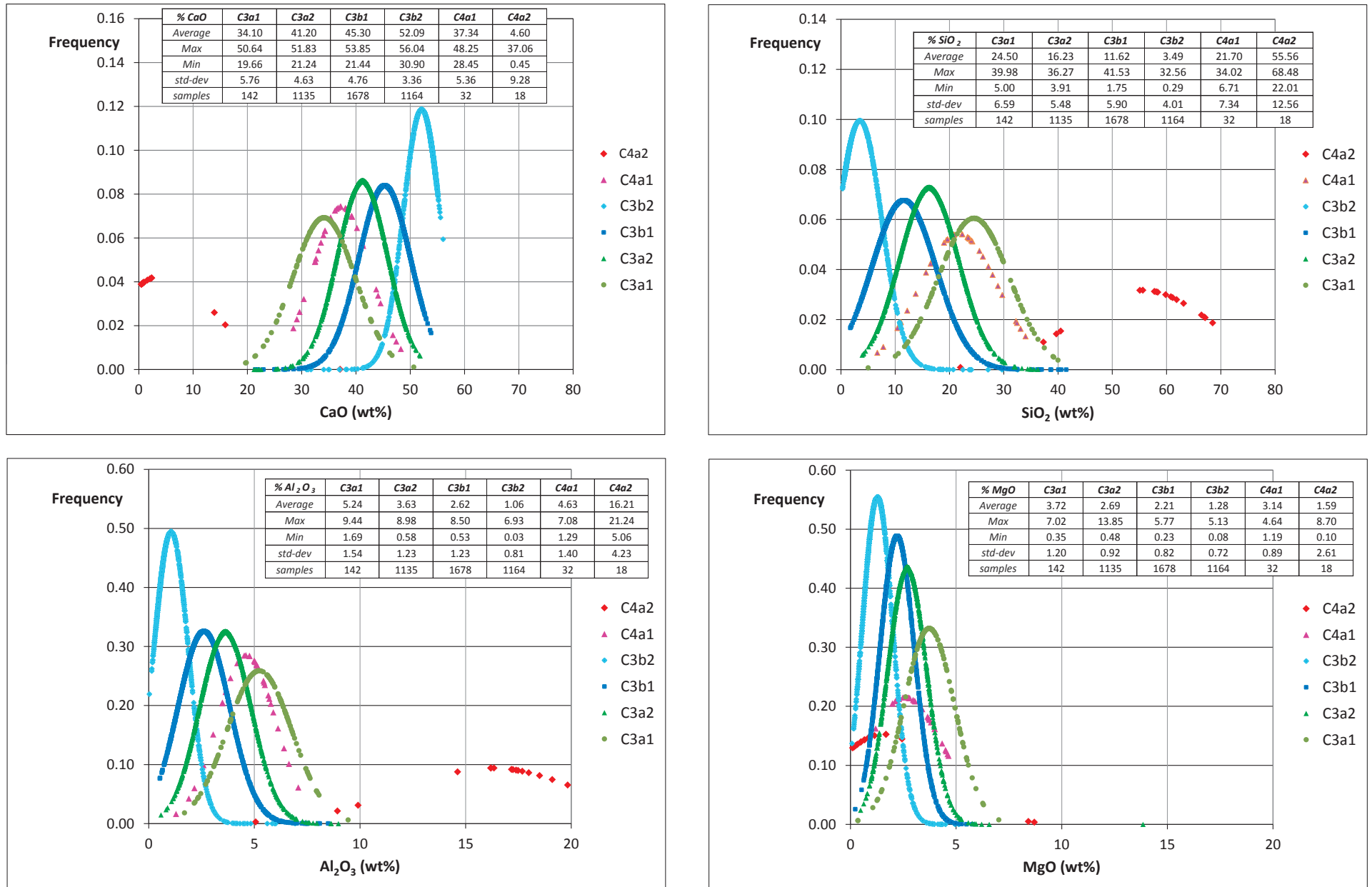
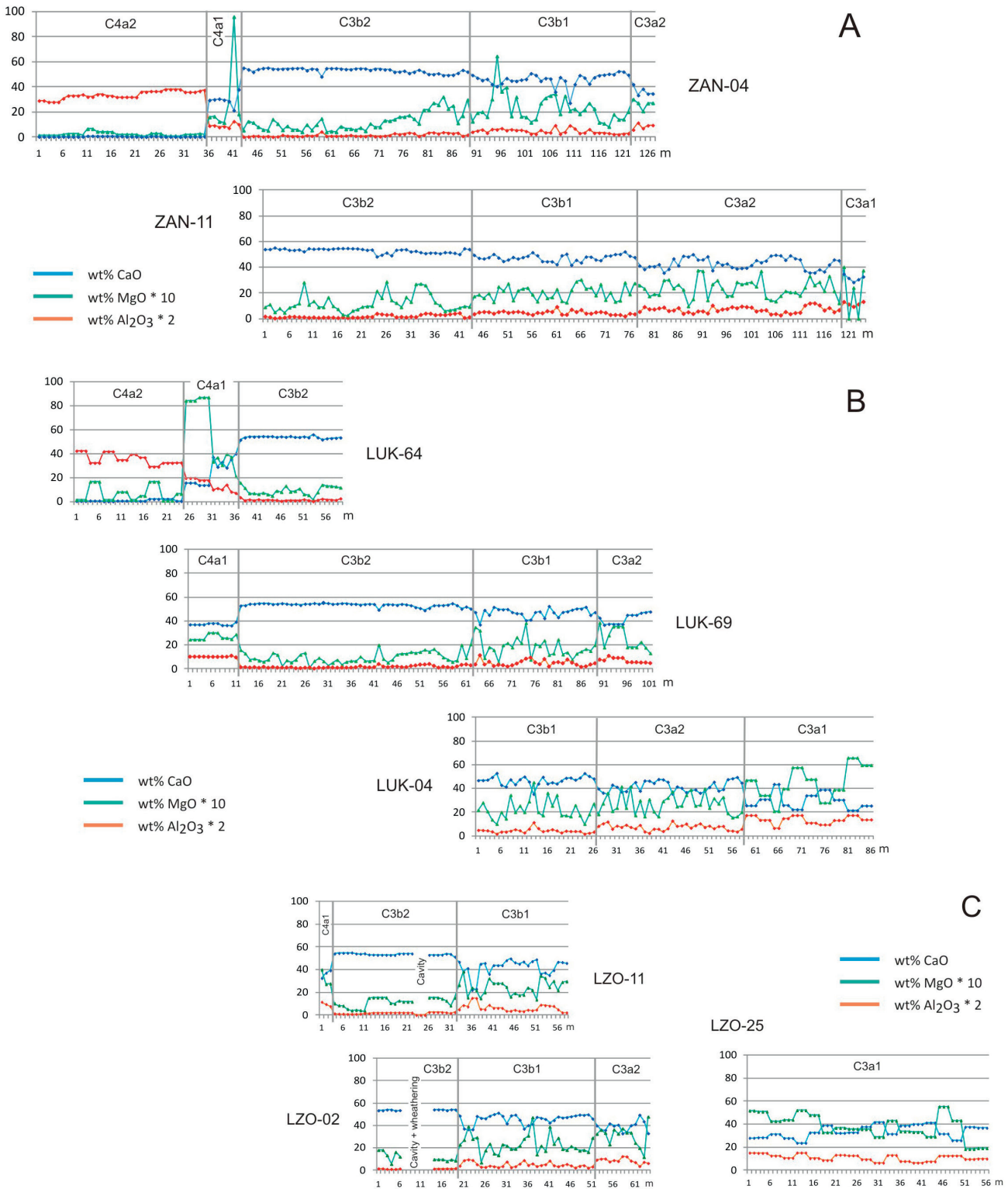


Figure 8. CaO (A), SiO<sub>2</sub> (B), Al<sub>2</sub>O<sub>3</sub> (C), and MgO (D) Gauss curves on the whole chemical dataset from the 2009-2012 exploration drilling for C3a1 up to C4a2 submembers.



**Figure 9.** CaO, MgO\*10 and Al<sub>2</sub>O<sub>3</sub>\*2 concentration curves for C3a1 up to C4a2 submembers from drill holes ZAN-04 and ZAN-11 for the Zanga zone (A), LUK-64, LUK-69 and LUK-04 for the Lukala zone (B), LZO-11, LZO-02 and LZO-25 for the Luzolo zone (C).

(Ca:Mg = 5.68 to 35.03; n = 32) and C4a2 (Ca:Mg = 0.50 to 20.85; n = 18) carbonates vary from dolomites to dolomitic limestones. By comparison, the C2 Formation displays dolomites to dolomitic limestones (Table 3C; Fig. 10B).

In conclusion, the dolomitic character appears highly variable in the whole succession studied, and is generally minor within the upper part of the C3 Formation.

#### 5.4. Carbon and oxygen isotopes

The new carbon and oxygen isotopes (Table 4A; Fig. 11) from the Zanga, Lukala and Luzolo zones give  $\delta^{13}\text{C}$  and  $\delta^{18}\text{O}$  values from -3.4 to -2.9‰ and -10.1 to -9.9‰, respectively, for the C3a1 submember (n = 2). The overlying C3a2 submember (n = 3)

ranges between -2.7 and -2.5‰ for  $\delta^{13}\text{C}$ , and between -10.7 and -10.2‰ for  $\delta^{18}\text{O}$ . These values are concordant with the isotopic data of the old CICO samples (n = 8), for which the  $\delta^{13}\text{C}$  and  $\delta^{18}\text{O}$  vary between -2.9 and -2.3‰, and between -10.5 and -8.1‰, respectively (Delpomdor et al., 2015). The  $\delta^{13}\text{C}$  and  $\delta^{18}\text{O}$  values for the C3b1 submember (n = 4) yield from -2.6 to -2.3‰, and -10.3 to -9.6‰, respectively, while the CICO values (n = 5) are slightly heaviest (-2.4 to -2.1‰ for  $\delta^{13}\text{C}$  and -9.7 to -9.1‰ for  $\delta^{18}\text{O}$ ). The  $\delta^{13}\text{C}$  isotope values for the C3b2 submember range between -2.5 and -1.5‰ for both new and CICO samples (n = 10), while the  $\delta^{18}\text{O}$  values slightly differ between the new (from -10.2 to -9.9‰; n = 4) and CICO samples (from -9.4 to -9.2‰; n = 6).

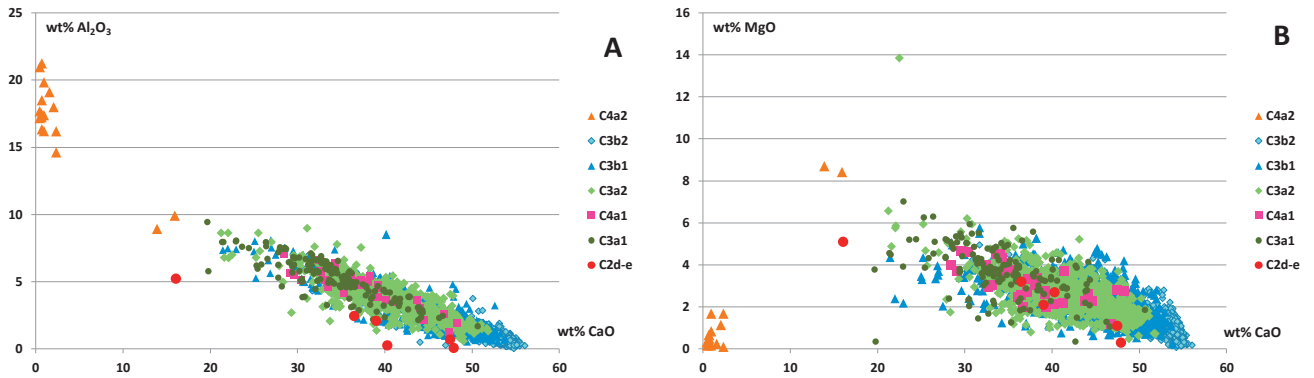


**Figure 10.** (A) CaO vs. Al<sub>2</sub>O<sub>3</sub> and (B) CaO vs. MgO concentration plots for C3a1 up to C4a2 submembers, and position of the C2 values from the old Kwilu-1, -2 and -S drill holes (Delpomdor et al., in revision).

In contrast, the C4a1-C4a2 submembers (n = 5) show a more large variation of  $\delta^{13}\text{C}$  and  $\delta^{18}\text{O}$  values, between -7.5 and -1.4‰, and between -7.8 and -5.6‰, respectively, suggesting a strong diagenetic alteration due to the presence of evaporites and/or to the dolomitization process.

The general trend of the  $\delta^{13}\text{C}$  isotope values within the Schisto-Calcaire Subgroup indicates an excursion to the negative

values in C1 and C2 units, and a progressive return to positive values from the C3 to the C5 units, with an abrupt decrease in the C4a1 submember (Tables 4A, 4B). Contrastingly, the  $\delta^{18}\text{O}$  values evolve in a more or less stable range from the C1 to the C3 units; higher values occur in the C4 and C5 units, especially in the C4a member, probably related to supratidal- to sabkha-type evaporitic environments as recorded by the lithological observations.

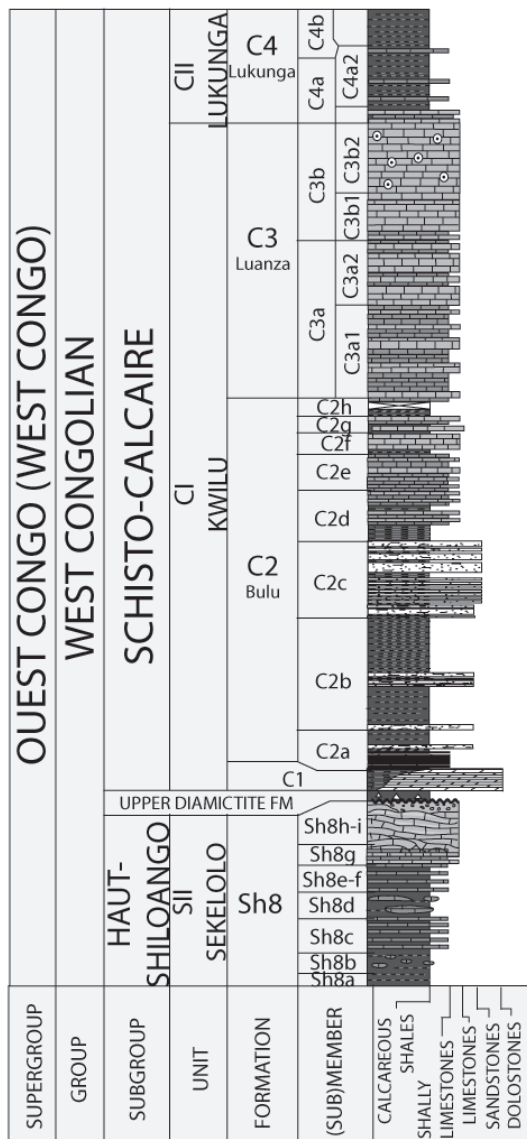


**Figure 11.** Composite litholog against  $\delta^{13}\text{C}$  and  $\delta^{18}\text{O}$  evolution from the top of the Haut-Shiloango Subgroup up to the basal C4 unit of the Schisto-Calcaire Subgroup (according to Frimmel et al., 2006; Straathof, 2011; Delpomdor & Pr at, 2013; Delpomdor et al., in revision; this paper).

## 6. Regional stratigraphic correlations

### 6.1. Intrabasinal correlation

The Schisto-Calcaire Subgroup rests unconformably on the 1 - 200 m Upper Diamictite Formation in the RC, DRC and Angola, and upon the Niari 'Tillite' Formation in Gabon. According to the 'Snowball Earth Hypothesis' stating the synchronous deposition of these diamictites, the Niari "Tillite" and the Upper Diamictite formations are thought to be related to the Marinoan glacial event (Tait et al., 2011).

In Gabon and RC, the Schisto-Calcaire Subgroup consists of four predominantly carbonate formations, called SCI to SCIV, respectively. The SCI dolomudstones Formation starts with a 6 - 12 m-thick basal member composed of cap-carbonate dolomites, showing  $\delta^{13}\text{C}$  mean values at -3.2‰ in Gabon (Préat et al., 2011) and -3.5‰ in RC (Préat et al., submitted) in the same order (-3.4‰) that the stratigraphically equivalent C1 unit in the DRC (Frimmel et al., 2006; Straathof, 2011; Delpomdor & Préat, 2013) (Tables 4B, 4C; Figs 11, 12).

$\delta^{13}\text{C}$  values analysed around -4.4‰ for the SCIC-a lithoherms and interstratified dolomites in Gabon (Préat et al., 2011), and between -4.07‰ and -2.77‰ (average of -3.75‰) for the SCIC peritidal dolomites in RC (Préat et al., submitted) suggest a correlation with the C2 unit in the DRC (average of -4.7‰) (Frimmel et al., 2006; Straathof, 2011; Delpomdor & Préat, 2013). The SCII and SCIII carbonates display an excursion from negative to positive  $\delta^{13}\text{C}$  values in the range of -3.3 to +6.3‰ in Gabon (Préat et al., 2011) and -3.74‰ to +8.36‰ in RC (Préat et al., submitted), comparable to values of the C4 and C5 formations in the DRC that vary between -7.5‰ and +12.6‰ (Tables 4B, 4C; Figs 11, 12) (Frimmel et al., 2006; Delpomdor & Préat, 2013). The  $\delta^{18}\text{O}$  values in Gabon and RC show a similar trend as for the equivalent units in DRC, but with a different order of values (Tables 4B, 4C; Figs 11, 12) (Frimmel et al., 2006; Straathof, 2011; Delpomdor & Préat, 2013).

The siliciclastic red-beds of the Schisto-Gréseux Group in Gabon and the Mpioka Group in RC that overlay unconformably the Schisto-Calcaire Subgroup, start with basal conglomerates, followed by rocks ranging from claystones to conglomeratic sandstones; they are correlated to the similar Mpioka Subgroup sequence in the DRC (Préat et al., 2011; Tait et al., 2011).

### 6.2. Regional correlation with the Central Africa Copperbelt

The WCB, Kaoko-Damara Belt (KDB) in Namibia and Central Africa Copperbelt (CAC) are Neoproterozoic sedimentary basins developed around the Congo craton as a consequence of the Rodinia supercontinent break up (Tack et al., 2001). Some litho-chronostratigraphical comparison or tentative global correlation between these sedimentary successions have already been sketched, based mainly on the occurrence of extensive diamictite formations related to the Sturtian and Marinoan glacial events (Cailteux & Misi, 2007; Poidevin, 2007; Kampunzu et al., 2009; Tack et al., 2001; Delpomdor & Préat, 2013). On one hand, the Mwale (Grand Conglomérat), Varianto (Chuons) and Lower Diamictite formations in the CAC, KDB and WCB, respectively, are all correlated with the 750-713 Ma global Sturtian glaciation (Key et al., 2001; Hoffman et al., 1996; Frimmel et al., 2006), and represent robust geochronological markers. On the other hand, similarly as for the younger Upper Diamictite Formation in the WCB, the Kyandamu (Petit Conglomérat) diamictite in the CAC is interpreted of the same age as for the  $\pm 635$  Ma Marinoan Ghaub diamictite in Namibia (Hoffmann et al., 2004; Kampunzu et al., 2009).

The mixed carbonate-siliciclastic lower sequence of the Nguba Group in the CAC, called Muombe Subgroup (up to 2500 m-thick), succeeds to the Mwale diamictite with a basal cap-carbonate (the Dolomie Tigrée, 0 to 50 m-thick), overlain by more or less calcareous to dolomitic carbonaceous shales or siltstones of the Kaponda Formation and by an open marine carbonate platform deposition of the Kakontwe Formation, ending with the more shallow Kipushi deposit (Batumike et al., 2007; Kampunzu et al., 2009). The overlying Bunkeya Subgroup forms an up to 3000 m-thick predominantly siliciclastic sequence prograding over

Submember		C3a1	C3a1	C3a2	C3a2	C3b1	C3b1	C3b1	C3b2	C3b2	C3b2	C4a1	C4a1	C4a1	C4a2
Lithology		ist.	ist.	ist.	ist.	ist.	ist.	ist.	ist.	ist.	ist.	ist.	ist.	ist.	ist.
Drill hole		ZAN-11	ZAN-23	ZAN-04	ZAN-04	ZAN-04	ZAN-04	ZAN-04	ZAN-04	ZAN-04	ZAN-04	LUK-64	LUK-64	LUK-64	LUK-64
Core		C.584	C.410	C.521	C.505	C.412	C.388	C.388bis	C.80	C.80bis	C.121	C.92bis	C.69	C.69bis	C.49
depth (m)		134.05	110.75	147.15	144.35	123.55	118.15	118.15	59.85	59.85	60.15	54.65	50.15	50.15	47.15
$\delta^{13}\text{C}_{\text{V-PDB}}$ (‰)		-3.4	-2.9	-2.7	-2.7	-2.4	-2.6	-2.3	-2.3	-2.2	-1.7	-1.4	-2.0	-2.4	-7.5
$\delta^{18}\text{O}_{\text{V-PDB}}$ (‰)		-10.1	-9.9	-10.7	-10.2	-10.3	-9.6	-9.8	-10.0	-9.9	-10.2	-5.9	-7.6	-7.8	-6.3
range $\delta^{13}\text{C}_{\text{V-PDB}}$ (‰)		-3.4 / -2.9 (n = 2)	-	-2.7 / -2.5 (n = 3)	-2.6 / -2.3 (n = 4)	-2.6 / -2.3 (n = 4)	-2.4 / -2.1 (n = 5)	-2.3 / -1.6 (n = 4)	-2.3 / -1.6 (n = 4)	-2.3 / -1.6 (n = 4)	-2.5 / -1.5 (n = 6)	-7.5 / -1.4 (n = 5)	-	-	-
range $\delta^{13}\text{C}$ (‰) CI-CO		-	-3.2	-2.9 / -2.3 (n = 8)	-2.6	-2.4 / -2.1 (n = 5)	-2.3	-1.9	-10.2 / -9.9 (n = 4)	-10.2 / -9.9 (n = 4)	-10.2 / -9.9 (n = 4)	-7.8 / -5.6 (n = 5)	-	-	-
range $\delta^{18}\text{O}_{\text{V-PDB}}$ (‰)		-10.1 / -9.9 (n = 2)	-	-10.7 / -10.2 (n = 3)	-10.5 / -8.1 (n = 8)	-9.7 / -9.1 (n = 5)	-9.7	-9.6	-9.4 / -9.2 (n = 6)	-9.4 / -9.2 (n = 6)	-9.6	-6.6	-	-	-
range $\delta^{18}\text{O}$ (‰) CI-CO		-	-10.0	-9.5	-9.5	-9.7	-9.7	-9.6	-9.6	-9.6	-9.6	-6.6	-	-	-
average $\delta^{18}\text{O}_{\text{V-PDB}}$ (‰)		-	-	-	-	-	-	-	-	-	-	-	-	-	-
n (number of samples)		2	2	11	11	9	9	9	10	10	10	5	5	5	5

Table 4. (A) New C and O isotope values for the C3 (Luanza) to C4 (Lukunga) formations from the new drill holes at Lukala (this paper).

**B - Schisto-Calcaire Subgroup in DRC (recent & new data)**

Formation/unit	U. D.	C1	C2	C3	C4	C5
Lithology	diamictite	cap-dol.	lst.	lst.	lst.	lst.
Drill hole (DH)/Quarry (Q)	Safricas Q & others	Safricas Q, SNEL, Kwilu	Kwilu-1,2,S, river & SNEL	CICO DH, Lukala DH+Q	Onatra & Mani Q, Lukala DH	BK, Ngufu Q, Kavuya Q
range $\delta^{13}C_{V-PDB}$ (‰)	+2.0/+6.3	-4.2 /-1.8	-5.8 /-3.1	-3.4 /-1.5	-7.5 /-0.1	+1.1 /+12.6
average $\delta^{13}C_{V-PDB}$ (‰)	+4.3	-3.1	-4.7	-2.3	-0.5	+6.3
range $\delta^{18}O_{V-PDB}$ (‰)	-11.6 /-7.6	-11.7 /-7.0	-12.4 /-9.4	-10.7 /-8.1	-10.6 /-2.4	-10.0 /-2.6
average $\delta^{18}O_{V-PDB}$ (‰)	-9.3	-9.4	-11.6	-9.6	-7.6	-6.1
n (number of samples)	4	78	32	45	30	28

**C - Schisto-Calcaire Subgroup in SW Gabon**

Formation/unit	SCIa	SCIc-a	SCI	SCII	SCIII
Lithology	cap-dol.	lithoherm			
Drill hole (DH)/Quarry (Q)	Ndende	Ndende	Ndindi, Tshobanga	Fougamou	Mouila Q
range $\delta^{13}C_{V-PDB}$ (‰)	-3.5 /-2.8	-4.9 /-3.6	-2.3 /+9.0	-3.3/+6.3	+1.0/+5.8
average $\delta^{13}C_{V-PDB}$ (‰)	-3.2	-4.4	+1.5	+1.1	+2.7
range $\delta^{18}O_{V-PDB}$ (‰)	-7.3 /-5.6	-9.8 /-5.9	-11.8 /-2.3	-8.6/+5.4	-5.1/-3.7
average $\delta^{18}O_{V-PDB}$ (‰)	-6.3	-9.1	-6.0	-3.9	-3.5
n (number of samples)	6	12	50	17	23

**D - São Francisco Basin (Brazil)**

Formation/unit	Jequitai/ Macaubas	Sete Lagoas	Sete Lagoas	Serra de Santa Helena	Lagoa do Jacaré
Lithology	diamictite	pink dol.	lst. & dol.	carbonates	carbonates
Location	Jequitai town area	Southern SFB	Rio de Janciro, Sete Lagoas & Jequitai areas	Rio de Janciro area	
range $\delta^{13}C_{PDB}$ (‰)	-7.7 /+2.1	-5.7 /-3.2	+1.1 /+16.1	+10.4 /+10.8	+10.4 /+14.7
average $\delta^{13}C$ (‰)	-1.9	-4.4	+9.2	+10.7	+11.7
range $\delta^{18}O_{PDB}$ (‰)	-14.4 /-6.4	-13.0 /-4.6	-15.4 /-4.9	-13.9 /-11.0	-12.6 /-9.5
average $\delta^{18}O$ (‰)	-10.1	-7.5	-7.6	-12.1	-11.0
n (number of samples)	36	16	107	3	8

Tables 4. (B) Compilation of recent C and O isotope values for the Schisto-Calcaire Subgroup in DRC (Delpomdor, 2007, Delpomdor & Pr at, 2011; Straathof, 2011; Delpomdor et al., 2014, 2015), (C) in SW Gabon (Pr at et al., 2011), and (D) for the SFB Bambu  Group in Brazil (Iyer et al., 1995; Santos et al., 2000, 2004).

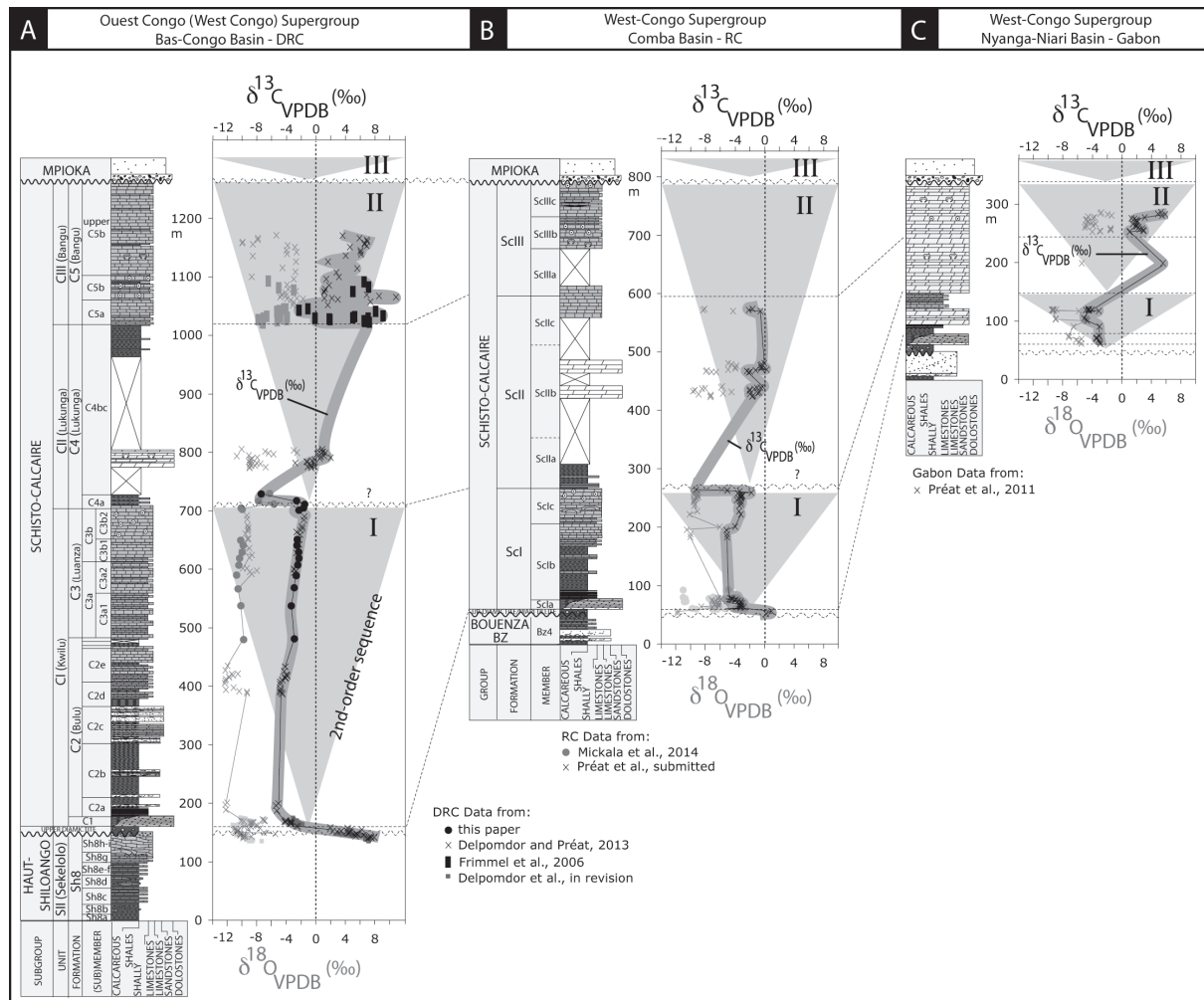


Figure 12. Composite litholog against  $\delta^{13}C$  evolution of the Schisto-Calcaire Subgroup correlated to the same units in RC and Gabon.

the carbonates. By comparison with the Bembezi and Sekelolo sequences of the Haut-Shiloango Subgroup, respectively, major differences occur. The Bembezi unit appears predominantly clastic, while the Sekelolo unit was recently interpreted as a short-time marine carbonate transgression on a passive margin, with open marine platform carbonate conditions (Delpomdor et al., 2014). The  $\delta^{13}\text{C}$  values are around +2.4‰, and between -4.3 and +2.8‰ (mean value +1.7‰) for the Kaponda and Kakontwe carbonate formations, respectively, to the bottom of the Nguba succession (Bull et al., 2011), and in the same trend between +2.4 and +8.0‰ (mean value +5.5‰) for the Sekelolo Formation in the WCB (Frimmel et al., 2006; Straathof, 2011; Delpomdor et al., 2014; Table 5; Fig. 13). The  $\delta^{18}\text{O}$  values for the same sequences are between -10.8 and -0.8‰ (mean value -2.8‰) for the Kaponda-Kakontwe formations, and between -12.1 and -4.7‰ (mean value -9.4‰) for the Sekelolo unit.

Succeeding to the Kyandamu diamictite in the CAC, interpreted of Marinoan age, the Gombela Subgroup starts with the basal 5 to 15 m-thick Lusele (Calcaire Rose) cap-carbonate, followed by up to 1600 m-thick alternating carbonatic shales and siltstones of the Kanianga Formation, and by up to 150 m-thick carbonate beds of the Lubudi Formation (Calcaire de Lubudi) at the top (Batumike et al., 2007). It displays a sedimentary succession strongly comparable to the C1, C2 and C3 formations of the Schisto-Calcaire, respectively (Table 6). In particular, the Lubudi Formation is marked by massive, irregularly bedded, oolitic high purity limestone beds alternating with sandy carbonate beds, showing shallow-water proximal conditions of deposition, similarly as for the C3b in Bas-Congo. Unfortunately, no carbon isotope values are available on the Lubudi limestone to support this correlation.

The overlying Mongwe and Kiubo formations up to > 600 m-thick are pelite-sandstone more or less dolomitic complexes, with frequent intraformational conglomerates and upward coarsening. The sequence contains predominant pelites to the bottom (Mongwe Formation), and predominant sandstones to the top (Kiubo Formation). These units are characterized by shallow-water and evaporitic conditions, similarly as for the C4 and C5 formations in Bas-Congo (Cahen, 1978). Youngest age for the C5 deposition suggested by strontium isotope ratios is ca. 550 Ma (Delpomdor & Pr eat, 2013), while thrusting of the folded Katangan terranes in CAC over the Mongwe-Kiubo sediments constrains the last deposition age for these formations in the range of 570-550 Ma (Kampunzu & Cailteux, 1999; Kipata et al., 2013). Sponge spicules and radiolaria Cambrian to present-day microfossils observed in chert beds of the Kiubo Formation (Cahen et al., 1946) also support this age.

Ending both successions (Table 6), the late-orogenic molasse-type Sampwe and Mpioka sequences deposited at  $\leq 573$  and  $\pm 566$  Ma in CAC and WCB, respectively (Tack et al., 2001; Master et al., 2005).

**Table 5.** Comparison of the C and O isotope values between the WCB Haut-Shiloango Subgroup (Frimmel et al., 2006; Straathof, 2011; Delpomdor & Pr eat, 2011) and the CAC Nguba Subgroup (Bull et al., 2011).

**A - West Congo Belt (DRC)**

Formation/unit	Lower Diamictite	Sekelolo
Lithology	diamictite	carbonates
Location		Safricas Quarry, RMCA, Lamba (Bas-Congo, DRC)
range $\delta^{13}\text{C}_{\text{V-PDB}}$ (‰)		+2.4 / +8.0
average $\delta^{13}\text{C}_{\text{V-PDB}}$ (‰)		+5.5
range $\delta^{18}\text{O}_{\text{V-PDB}}$ (‰)	?	-12.1 / -4.7
average $\delta^{18}\text{O}_{\text{V-PDB}}$ (‰)		-9.4
n (number of samples)		80

**B - Central Africa Copperbelt (DRC)**

Formation/unit	Mwale	Dol. Tigr�e ?	Kakontwe
Lithology	diamictite	cap-dol	dol. & lst.
Drill Hole (DH)	DH. Itawa 26	DH. Itawa 26	DH. Itawa 26
Location	Zambia	Zambia	Zambia
range $\delta^{13}\text{C}_{\text{PDB}}$ (‰)	-6.0 / -4.6	+2.3 / +2.5	-4.3 / +2.8
average $\delta^{13}\text{C}_{\text{PDB}}$ (‰)	-5.3	+2.4	+1.7
range $\delta^{18}\text{O}_{\text{PDB}}$ (‰)	-8.4 / -7.2	-4.0 / -3.8	-10.8 / -0.8
average $\delta^{18}\text{O}_{\text{PDB}}$ (‰)	-7.8	-3.9	-2.8
n (number of samples)	2	2	38

At the top of the CAC succession, the tabular Bianco Subgroup (> 400 m-thick) is a deposit younger than and unrelated to the Lufilian (Pan-African) orogeny, probably of Palaeozoic Karoo age (Dumont et al., 1997; Batumike et al., 2007; Kampunzu et al., 2009). This is in agreement with the post-Karoo transpressional structural inversion (D3 Chilatembo stage of Kampunzu & Cailteux, 1999) that affected the Bianco succession (Kipata et al., 2013). Therefore, this last has to be separated from the Kundelungu Group and considered as an individual lithostratigraphic unit similarly as for the tabular Inkisi deposit in the WCB (Tack et al., 2001).

**6.3. Regional correlations with the S o Francisco basin (SFB)**

The Neoproterozoic sedimentary rocks of the Bambu  Group in Brazil form a 450 - 1800 m-thick transgressive sequence over the S o Francisco craton on an intracontinental platform in relatively shallow water conditions. The Bambu  Group occurs along the south-eastern margin of the S o Francisco Basin, overlying the Maca bas Group/Jequitai Formation diamictites (Pflug & Sch ll, 1975; Karfunkel & Karfunkel, 1975; Karfunkel & Hoppe, 1988) that are interpreted of Sturtian age (Santos et al., 2000, 2004; Babinski et al., 2007). Along the southern margin of the SFB, these diamictites pass laterally to the Carrancas Formation (Uhlein et al., 2012). According to Dardenne (1978), the Bambu  Group is divided into five units, from oldest to youngest: (1) the Sete Lagoas Formation, composed of 500 m-thick limestones and dolostones interbedded with shales, (2) the Serra de Santa Helena Formation, which comprises  $\pm 600$  m-thick thin-bedded shales and siltstones with interbeds of limestones and sandstones, (3) the Lagoa do Jacar  Formation, mainly composed of 350 m-thick limestones with oolites and stromatolites overlain by calcareous siltstones and shales, (4) the Serra da Saudade Formation, mainly composed of approximately 200 m-thick silty shales and shales with interbeds of shaly limestones, and (5) the Tr s Marias Formation, 300-400 m-thick, dominantly composed of arkoses, lithic sandstones and siltstones. Furthermore, the Sete Lagoas Formation is marked by: (1) a regional unconformity located into the post-Sturtian Pedro Leopoldo Member, which consists of shaly limestones capped by dolomites with a Pb-Pb age of  $742 \pm 22$  Ma (Babinski et al., 2007), and (2) a post-Marinoan Lagoa Santa Member dominantly composed of limestones. However, refuting this gap of time, Paula-Santos et al. (2015) proposed a new maximum U-Pb age of  $593 \pm 17$  Ma based on detrital zircon grains from the Pedro Leopoldo Member. Youngest detrital zircon population for most of the Sete Lagoas formations gave a depositional age of 557 Ma (Babinski et al., 2013), which is supported by the occurrences of Claudina late Ediacaran fossils recently found in the uppermost Sete Lagoas Formation (Warren et al., 2014). Nevertheless, the ages for the Bambu  Group are still debated, the maximum depositional age for the Bambu  Group being considered around 600 Ma (Rodrigues, 2008).



In this paper, the West Congolian Group is attempted to be correlated with the Bambuí Group using the chemostratigraphic tool.

The  $\delta^{13}\text{C}$  pattern of the Macaúbas Group displays isotopic variations (Table 4D), which evolve from between -7.7 and +2.1‰ in the Jequitai diamicite, and between -4.2 and -3.7‰ in the Carrancas diamicite. In the overlying Bambuí Group it varies between -5.7 and -3.2‰ in a basal dolomite of the Sete Lagoas Formation (Alvarenga et al., 2007; Kuchenbecker, 2011; Caxito et al., 2012) that probably corresponds to a cap-carbonate after the Jequitai/Carrancas diamicites (Fig. 14). The carbon isotope increases between +1.1 and +16.1‰ values in the upper part of the Sete Lagoas carbonates, and remains with high values between +10.4 and +14.7‰ in the Serra de Santa Helena and Lagoa do Jacaré formations (Iyer et al., 1995; Santos et al., 2000; Misi et al., 2007).

This  $\delta^{13}\text{C}$  profile is similar to those of the Schisto-Calcaire Subgroup in DRC, which displays a comparable negative shift in the Upper Diamicite and C1 formations, and an upwards increase from very negative values from the base of the C2 Formation,

passing by a second negative shift in  $\delta^{13}\text{C}$  at the C3/C4 formations transition, towards positive values in the C5 Formation (Tables 4B, 4D; Fig. 14). The C3/C4 formations transition is clearly highlighted by abrupt lithological and chemical changes, related to the gradual regional-scale return for a predominantly clastic system mixed with short-time evaporitic lagoon-type lime depositions at the base of a second marine transgression, after a possible long period of non-deposition and/or karstification, in the basin. This 2<sup>nd</sup>-order transgressive sequence is repeated from the C4 to C5 formations, which are overlain by a third 2<sup>nd</sup>-order sequence composed by the Mpioika Subgroup (Delpomdor, 2015, unpublished). Similarly, the Bambuí Group can be also subdivided into three 2<sup>nd</sup>-order sequences, which comprise from base to top: (1) the Sete Lagoas Formation, (2) the Serra de Santa Helena and Lagoa do Jacaré formations, and (3) the Serra da Saudade and Três Marias formations (Alkmim & Martins-Neto, 2012; Fig. 14). As a result, both the isotopic chemostratigraphy and lithostratigraphy suggest a regional correlation between the 2<sup>nd</sup>-order sequences of the SFB in Brazil and of the WCB in DRC-RC-Gabon as follows: (1) Sete Lagoas Formation and

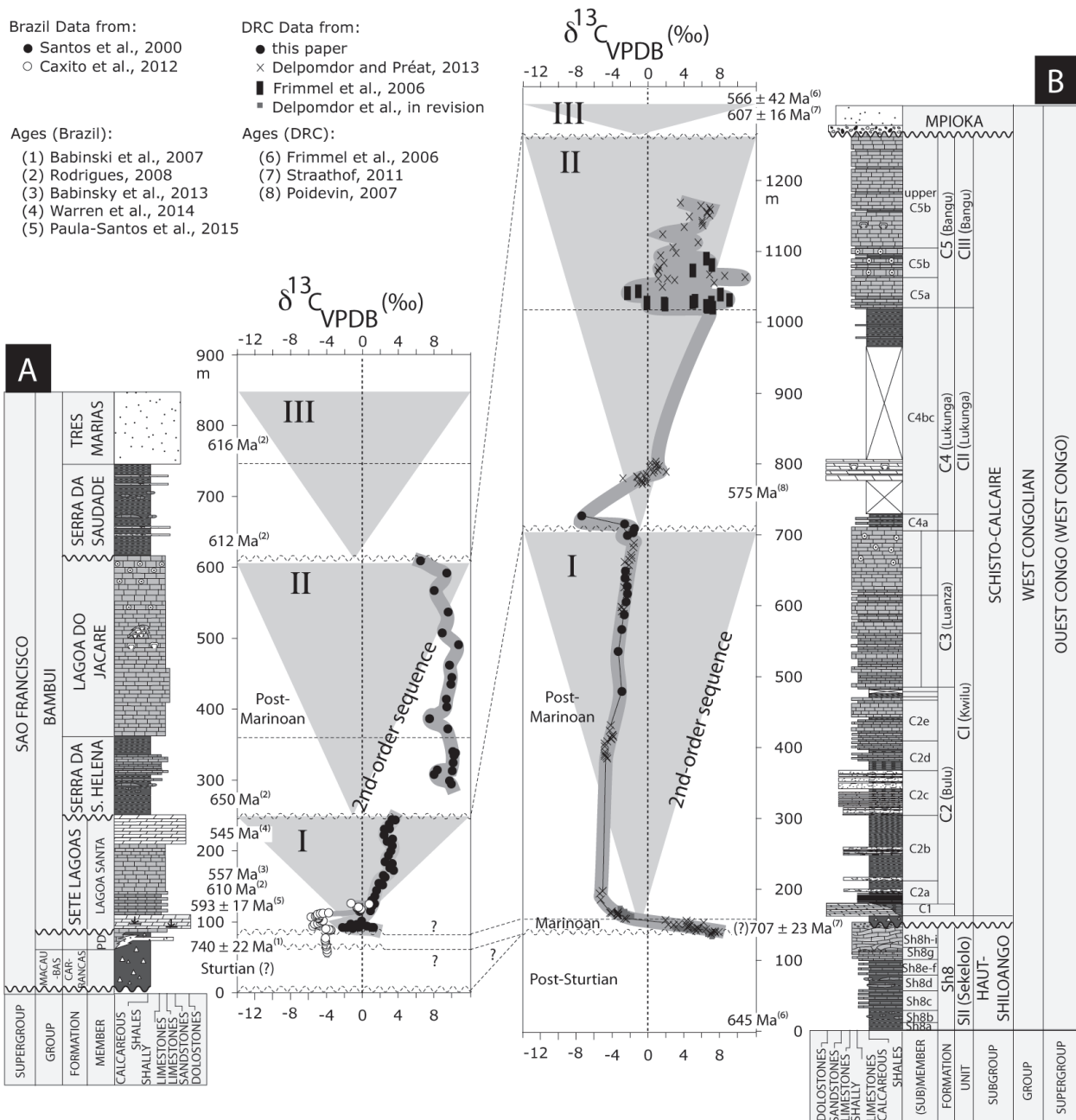


**Figure 14.** Composite litholog against  $\delta^{13}\text{C}$  evolution of the Schisto-Calcaire subgroup compared to the Bambuí Group in the SFB (Brazil). Abbreviations: PD, Pedro Leopoldo Member.



overall in these basins, and are used as tool of correlation partly in association with chemostratigraphy. The Sete Lagoas - C1/C3 - Kanianga/Lubudi formations, the Serra de Santa Helena and Lagoa do Jacaré - C4/C5 - Mongwe/Kiubo formations, and finally the Serra da Saudade and Três Marias formations - Mpioka - Sampwe subgroups can be regionally correlated between the São Francisco Basin in Brazil, the West Congo Basin in DRC-RC-Gabon and the Central Africa Copperbelt in DRC (Table 6).

The tabular Inkisi (WCB) and Bianco (CAC) successions that have to be considered as individual lithostratigraphic units, are supposedly correlated to Karoo age, but no time constraints occur to confirm this correlation.

## 8. Acknowledgements

The Forrest Group and Heidelberg Cement Companies are thanked for their agreement in publication of drill core logs and chemical results. The geochemical as well as the O and C isotope analyses were carried out at the University of Erlangen in Germany (Prof. Michael Joachimski). We also thank the Royal Museum for Central Africa (RMCA) for the access to the CICO available cores. We are grateful to Prof. Philippe Muchez and Dr. Stefan Schroeder for their constructive reviews.

## 9. References

- Alkmim, F.F. & Martins-Neto, M.A., 2012. Proterozoic first-order sedimentary sequences of the Sao Francisco craton, eastern Brazil. *Marine and Petroleum Geology* 33, 127-139.
- Allen, M.B., Jones, S., Ismail-Zadeh, A., Simmons, M. & Anderson, L., 2002. Onset of subduction as the cause of rapid Pliocene-Quaternary subsidence in the South Caspian basin. *Geology* 30, 775-778.
- Alvarenga, C.J.S., Della Giustina, M.E.S., Silva, M.G.C., Santos, R.V., Gioia, S.M.C., Guimarães, E.M., Dardenne, M.A., Sial, A.N. & Ferreira, V.P., 2007. Variações dos isótopos de C e Sr em carbonatos pré e pós-glaciác, ão Jequitaiá (Esturtiano) na região de Bezerra-Formosa, Goiás. *Revista Brasileira de Geociências* 37, 147-155.
- Alvarez, P., 1992. Répartition de la sédimentation dans le golfe Protérozoïque supérieur du Schisto-calcaire au Congo et Gabon. Implications en Afrique centrale. *Palaeogeography, Palaeoclimatology, Palaeoecology* 96, 281-297.
- Alvarez, P., 1995. Evidence for a Neoproterozoic carbonate ramp on the northern edge of the Central Africa Craton: relations with Late Proterozoic intracratonic troughs. *Geologische Rundschau* 84, 636-648.
- Alvarez, P. & Maurin, J.-C., 1991. Evolution sédimentaire et tectonique du bassin protérozoïque supérieur de Comba (Congo): stratigraphie séquentielle du Supergroupe Ouest-Congolien et modèle d'amortissement sur décrochements dans le contexte de la tectogénèse panafricaine. *Precambrian Research* 50, 137-171.
- Babinski, M., Vieira, L.C. & Trindade, R.I.F., 2007. Direct dating of the Sete Lagoas Cap Carbonate (Bambuï Group, Brazil), and implications for Neoproterozoic glacial events. *Terra Nova* 19, 1-6.
- Babinski, M., Paula-Santos, G.M., Kuchenbecker, M., Caetano-Filho, S., Trindade, R.I. & Pedrosa-Soares, A.C., 2013. The isotopic record of the Bambuï Group, Brazil: Sturtian, Marinoan, and/or Early Paleozoic? American Geophysical Union Spring Meeting Abstracts.
- Batunike, M.J., Cailteux, J.L.H. & Kampunzu, A.B., 2007. The Neoproterozoic Nguba and Kundelungu successions in the central African Copperbelt: lithostratigraphy, basin development and regional correlations. *Gondwana Research* 11, 432-447.
- Bertrand-Sarfati, J. & Milandou, R., 1989. Mécanismes de croissance des stromatolites géants infralittoraux, Protérozoïque supérieur du Congo. *Bulletin de la Société Géologique de France* 8, 1185-1192.
- Borg, G., Kämer, K., Buxton, M., Armstrong, R. & Van Der Merwe, S.W., 2003. Geology of the Skorpion zinc deposit, southern Namibia. *Economic Geology* 98, 749-771.
- Brito-Neves B.B., Campos-Neto M.C. & Fuck R.A., 1999. From Rodinia to Western Gondwana: An approach to the Brasiliano-Pan African cycle and orogenic collage. *Episodes* 22, 155-199.
- Bull, S., Selley, D., Broughton, D., Hitzman, M., Cailteux, J., Large, R. & McGoldrick, P. 2011. Sequence and carbon isotopic stratigraphy of the Neoproterozoic Roan Group strata of the Zambian copperbelt. *Precambrian Research* 190, 70-89.
- Cahen, L., 1954. Géologie du Congo Belge. Vaillant-Carmanne, Liège.
- Cahen, L., 1978. La stratigraphie et la tectonique du Supergroupe Ouest-Congolien dans les zones médiane et externe de l'orogène Ouest-Congolien (Pan-Africain) au Bas-Zaïre et dans les régions voisines. *Annales du Musée royal de l'Afrique Centrale, Tervuren*, in 8°, *Sciences Géologiques* 83, 1-150.
- Cahen, L. & Lepersonne, J., 1976. Les mixites du Bas-Zaïre: mise au point intérimaire. Musée royal de l'Afrique Centrale, Tervuren (Belgique), Département de Géologie et Minéralogie, Rapport annuel 1975, 33-57.
- Cahen, L., Jamotte, A. & Mortelmans, G., 1946. Sur l'existence de microfossiles dans l'horizon des cherts du Kundelungu Supérieur. *Annales de la Société Géologique de Belgique*, 70, B55-B65.
- Cailteux, J.L.H. & Misi, A., 2007. Neoproterozoic sediment-hosted base metal deposits of Western Gondwana. *Gondwana Research* 11, 344-345.
- Caxito, F.A., Halverson, G.P., Uhlein, A., Stevenson, R., Dias, T.G. & Uhlein, G.J., 2012. Marinoan glaciation in east central Brazil. *Precambrian Research* 200-203, 38-58.
- Chilingar, G.V., 1957. Classification of limestones and dolomites on basis of Ca/Mg ratio. *Journal of Sedimentary Petrology* 27, 187-189.
- Chilingar, G.V., 1960. Notes on classification of limestones and dolomites on basis of chemical composition. *Journal of Sedimentary Petrology* 30, 157-158.
- Cordani, U.G., Brito-Neves, B.B., D'Agrella, M.S. & Trindade, R.I.F., 2003. Tearing-up Rodinia: the Neoproterozoic paleogeography of North American cratonic fragments. *Terra Nova* 15, 343-349.
- Cosson, J., 1955. Notice explicative sur les feuilles de Pointe-Noire et Brazzaville. Carte géologique de reconnaissance au 1/500.000°. Direction des Mines et de la Géologie, Afrique Equatoriale Française, Brazzaville, 56 p.
- Dardenne, M.A., 1978. Sintese sobre a estratigrafia do Grupo Bambuï no Brasil Central. In: *Anais do 30<sup>th</sup> Congresso Brasileiro de Geologia*. Recife 1978. Recife, vol. 2. Sociedade Brasileira de Geologia, 507-610.
- Delhay, F. & Sluys, M., 1920. Les grands traits de la tectonique du Congo occidental. Structure et stratigraphie du bassin schisto-calcaireux (Note préliminaire). *Annales de la Société Géologique de Belgique, Publications relatives au Congo Belge* 43, C57-C74.
- Delhay, F. & Sluys, M., 1923. Esquisse géologique du Congo occidental. Etude du système Schisto-Calcaire; missions géologiques de 1914 et 1918-19. Bruxelles-Uccle. Etablissement Cartographique E. Patesson, 1923-1924.
- Delhay, F. & Sluys, M., 1924a. Observations ayant servi à l'élaboration de l'Esquisse géologique du Congo occidental. Etude du système schisto-calcaire (Echelle de 1/200.000, Missions géologiques de 1914 et 1918-1919). Premier mémoire: La région plissée des abords du fleuve, entre Isangila et Manyanga. *Annales de la Société Géologique de Belgique, Publications relatives au Congo Belge* 47, C50-C148.
- Delhay, F. & Sluys, M., 1924b. Observations ayant servi à l'élaboration de l'Esquisse géologique du Congo occidental. Etude du système schisto-calcaire (Echelle de 1/200.000, Missions géologiques de 1914 et 1918-1919). Deuxième mémoire: Le massif de Kikenge et la région effondrée du bassin de la Lua. *Annales de la Société Géologique de Belgique, Publications relatives au Congo Belge* 47, C149-C191.
- Delhay, F. & Sluys, M., 1929. Observations ayant servi à l'élaboration de l'Esquisse géologique du Congo occidental. Etude du système schisto-calcaire (Echelle de 1/200.000, Missions géologiques de 1914 et 1918-1919). Troisième mémoire: La région des plaines calcaires et les parties limitrophes au sud du fleuve dans la zone des plissements. Les observations faites le long de la ligne du chemin de fer. Le plateau schisto-gréseux des Cataractes-nord. *Annales de la Société Géologique de Belgique, Publications relatives au Congo Belge* 52, C69-C114.
- Delpomdor, F., 2007. Lithostratigraphie et sédimentologie de la chaîne Ouest Congolienne du Néoproterozoïque supérieur (Formation de la Diamictite supérieure et Sous-groupe du Schisto-Calcaire) Bas-Congo, République Démocratique du Congo. Unpublished MSc thesis, Université libre de Bruxelles, Belgium, 138 p.
- Delpomdor, F., 2015. The carbonates of the West Congo Supergroup – An example of glacio-eustatism related to short-time tectonic events on the western margin of the Congo Craton. Meeting, Universidade Federal de Minas Gerais, Belo Horizonte, Brazil, unpublished.
- Delpomdor, F. & Prêat, A., 2013. Early and late Neoproterozoic C, O and Sr isotope chemostratigraphy in the carbonates of West Congo and Mbuji-Mayi supergroups: A preserved marine signature? *Palaeogeography, Palaeoclimatology, Palaeoecology* 389, 35-47.
- Delpomdor, F., Kant, F. & Prêat, A., 2014. Neoproterozoic uppermost Haut-Shiloango Subgroup (West Congo Supergroup, Democratic Republic of Congo): misinterpreted stromatolites and implications for sea-level fluctuations before the onset of the Marinoan glaciation. *Journal of African Earth Sciences* 90, 49-63.
- Delpomdor, F., Tack, L., Cailteux, J. & Prêat, A., 2015. The C2 and C3 formations of the Schisto-Calcaire Subgroup (West Congo Supergroup) in the Democratic Republic of the Congo: An example of post-Marinoan sea-level fluctuations as a result of extensional tectonisms. *Journal of African Earth Sciences* 110, 14-33.

- Delpomdor, F., Eyles, N., Tack, L. & Pr at, A., in revision. West-Congolian pre- and post-Marinoan carbonates in the Democratic Republic of Congo: glacially- or tectonically-influenced deep-water sediments. *Precambrian Research*.
- De Paepe, P., Hertogen, J. & Tack, L., 1975. Mise en  vidence de laves en coussin dans les faci s volcaniques basiques du massif de Kibungu (Bas-Za re) et implications pour le magmatisme ouest-congolien. *Annales de la Soci t  G ologique de Belgique* 98, 251-270.
- Dumont, P., Hanon, M. & Ngoyi, L.K., 1997. La structure g ologique du plateau des Biano (Shaba, Za re). Mus e royal de l'Afrique Centrale, Tervuren (Belgique), D partement de G ologie et de Min ralogie, Rapport annuel 1995 et 1996, 169-182.
- Dunham, R.J., 1971. Meniscus cement. In: Bricker, O.P., (ed.), *Carbonate cements*. American Association of Petroleum Geologists, study in geology n 19. Johns Hopkins University Press, Baltimore, 297-300.
- Dupont, H., 1971. Etudes g ologiques en vue de rechercher et  valuer des mati res premi res pour l'usine CICO   Lukala. DP/71/2097/HD/IS.
- Dupont, H., 1972. Lev  de la carte g ologique de la r gion de Lukala. Soci t  des Ciments du Za re, Lukala. DP/72/0161/HD/IS.
- Frimmel, H.E., Hartnady, C.J.H. & Koller, F., 1996. Geochemistry and tectonic setting of magmatic units in the Pan-African Gariep Belt, Namibia. *Chemical Geology* 130, 101-121.
- Frimmel, H.E., Tack, L., Basei, M.S., Nutman, A.P. & Boven, A., 2006. Provenance and chemostratigraphy of the Neoproterozoic West Congolian Group in the Democratic Republic of Congo. *Journal of African Earth Sciences* 46, 221-239.
- Hanson, R.E., 2003. Proterozoic geochronology and tectonic evolution of southern Africa. In: Yoshida, M., Windley, B.F., Dasgupta, S., (eds), *Proterozoic East Gondwana: Supercontinent assembly and breakup*. Geological Society of London Special Publication 206, 427-463.
- Hoffman, P.F. & Schrag, D.P., 2002. The snowball Earth hypothesis: Testing the limits of global change. *Terra Nova* 14, 129-155.
- Hoffman, P.F., Hawkins, D.P., Isachsen, C.E. & Bowring, S.A., 1996. Precise U-Pb zircon ages for early Damaran magmatism in the Summas Mountains and Welwitschia Inlier, northern Damara belt, Namibia. *Communications of the Geological Survey of Namibia* 11, 47-55.
- Hoffman, P.F., Kaufman, A.J., Halverson, G.P. & Schrag, D.P., 1998. A Neoproterozoic snowball Earth. *Science* 281, 1342-1376.
- Hoffmann, K.-H., Condon, D.J., Bowring, S.A. & Crowley, J.L., 2004. U-Pb zircon date for the Neoproterozoic Ghaub Formation, Namibia: constraints on Marinoan glaciation. *Geology* 32, 817-820.
- Iyer, S.S., Babinski, M., Krouse, H.L. & Chemale, F., 1995. Highly <sup>13</sup>C enriched carbonate and organic matter in the Neoproterozoic sediments of the Bambui Group, Brazil. *Precambrian Research* 73, 271-282.
- Jauniau, F. & Dujardin, A., 1970. Etude du gisement de Mingwangwa, Rapport n 2: Lev  g ologique   Mingwangwa. Soci t  des Ciments du Congo, Lukala, DP/70/1563/FJ/IS.
- Kadima, E., Delvaux, D., Sebagenzi, S.N., Tack, L. & Kabeya, S.M., 2011. Structure and geological history of the Congo Basin: an integrated interpretation of gravity, magnetic and reflection seismic data. *Basin Research* 23, 499-527.
- Kampunzu, A.B. & Cailteux, J., 1999. Tectonic evolution of the Lufilian Arc (Central Africa Copper Belt) during Neoproterozoic pan African orogenesis. *Gondwana Research* 2, 401-421.
- Kampunzu, A.B., Cailteux, J.L.H., Kamona, A.F., Intiomale, M.M. & Melcher, F., 2009. Sediment-hosted Zn-Pb-Cu deposits in the Central African Copperbelt. *Ore Geology Reviews* 35, 263-297.
- Karfunkel, J. & Hoppe, A., 1988. Late Proterozoic glaciation in central-eastern Brazil: synthesis and model. *Palaeogeography, Palaeoclimatology, Palaeoecology* 65, 1-21.
- Karfunkel, B. & Karfunkel, J., 1975. Fazielle Entwicklung der mittleren Espinha o-Zone mit besonderer Ber cksichtigung des Tillit Problems (Minas Gerais/Brasilien). Unpublished PhD. Thesis, University of Freiburg, Germany, 86 p.
- Key, R.M., Liyungu, A.K., Njamu, F.M., Somwe, V., Banda, J., Mosley, P.N. & Armstrong, R.A., 2001. The western end of the Lufilian Arc in NW Zambia and its potential for copper deposits. *Journal of African Earth Sciences* 33, 503-528.
- Kipata, M.L., Delvaux, D., Sebagenzi, M.N., Cailteux, J. & Sintubin, M., 2013. Brittle tectonic and stress field evolution in the Pan-African Lufilian arc and its foreland (Katanga, DRC): from orogenic compression to extensional collapse, transpressional inversion and transition to rifting. *Geologica Belgica* 16, 1-17.
- Kirschvink, J.L., 1992. Late Proterozoic low-latitude global glaciation: the snowball Earth. In: Schopf, J.W., Klein, C., (eds), *The Proterozoic biosphere: a multidisciplinary study*. Cambridge University Press, Cambridge, 51-52.
- Kr ner, A. & Stern, R.J., 2005. Pan-African orogeny. In: Selley, R.C., Cocks, L.R.M., Plimer, I.R., (eds), *Encyclopedia of Geology*. Vol. 1, A-En. Elsevier, Amsterdam, 1-12.
- Kuchenbecker, M., 2011. Quimioestratigrafia e proveni ncia sedimentar da por o basal do Grupo Bambui em Arcos (MG). Masters Dissertation, IGC-Universidade Federal de Minas Gerais, Belo Horizonte, Brazil, 91 p.
- Lepersonne, J., 1974. Carte g ologique   l' chelle 1/200000. Notice explicative de la feuille Ngungu (Degr  carr  S6/14 = SB 33.9). R publique D mocratique du Congo. D partement des Mines, Direction du Service G ologique, 61 p.
- Martins-Neto, M.A., 2009. Sequence stratigraphic framework of Proterozoic successions in eastern Brazil. *Marine and Petroleum Geology* 26, 163-176.
- Master, S., Rainaud, C., Armstrong, R.A., Phillips, D. & Robb, L.J., 2005. Provenance ages of the Neoproterozoic Katanga Supergroup (Central African Copperbelt), with implications for basin evolution. *Journal of African Earth Sciences*, 42, 41-60.
- Mayor, H., 1951. Observations in dites. Syndicat BAMOCO.
- Mickala, O.-R., Vidal, L., Boudzoumou, F., Affaton, P., Vandamme, D., Borschneck, D., Moo-ungengui, M.M., Fournier, F., Nmaloungula Nganga, D.M. & Miche, H., 2014. Geochemical characterization of the Marinoan 'Cap Carbonate' of the Niari-Nyanga Basin (Central Africa). *Precambrian Research* 255 (1), 367-380.
- Misi, A., Kaufman, A.J., Veizer, J., Powis, K., Azmy, K., Boggiani, P.C., Gaucher, C., Teixeira, J.B.G., Sanches, A.L. & Iyer, S.S., 2007. Chemostratigraphic correlation of Neoproterozoic successions in South America. *Chemical Geology* 237, 143-167.
- Moore, C.H., 1989. Carbonate diagenesis and porosity. Amsterdam, Elsevier.
- Moore, C.H. & Druckman, Y., 1981. Burial diagenesis and porosity evolution, Upper Jurassic Smackover, Arkansas and Louisiana. *American Association of Petroleum Geologist Bulletin* 65, 597-628.
- Nicolini, P., 1959. Le synclinal de la Nyanga (zone de la boucle du Niari). Contribution   l' tude des min ralisations stratiformes du Moyen-Congo. *Bulletin de la Direction des Mines et de la G ologie, Afrique Equatoriale Fran aise* 10, 178 p.
- Paula-Santos, G.M., Babinski, M., Kuchenbecker, M., Caetano-Filho, S., Trindade, R.I. & Pedrosa-Soares, A.C., 2015. New evidence of an Ediacaran age for the Bambui Group in southern S o Francisco craton (eastern Brazil) from zircon U-Pb data and isotope chemostratigraphy. *Gondwana Research* 28 (2), 702-720.
- Pedrosa-Soares, A.C., Babinski, M., Noce, C., Martins, M.S., Queiroga, G. & Vilela, F., 2011. The Neoproterozoic Macatibas Group (Araua  orogen, SE Brazil) with emphasis on the diamictite formations. In: Arnaud, E., Halverson, G. & Shields, G., (eds), *The geological record of Neoproterozoic glaciations*, Geological Society of London, Memoir 36, 523-534.
- Pflug, R. & Sch ll, W.U., 1975. Proterozoic glaciation in Eastern Brazil: a review. *Geologische Rundschau* 64, 287-299.
- Poidevin, J.-L., 2007. Stratigraphie isotopique du strontium et datation des formations carbonat es et glaciog niques n oproterozo ques du Nord et de l'Ouest du craton du Congo. *Comptes Rendus Geoscience* 339, 259-273.
- Pr at, A., Prian, J.P., Thi blemont, D., Mabicka Obame, R. & Delpomdor, F., 2011. Stable isotopes of oxygen and carbon compositions in the Neoproterozoic of South Gabon (Schisto-Calcaire Subgroup, Nyanga Basin): Are cap carbonates and lithoherms recording a particular destabilization event after the Marinoan glaciation? *Journal of African Earth Sciences* 60, 273-287.
- Pr at, A., Delpomdor, F. & Callec, Y., submitted. Palaeoenvironments,  $\delta^{13}\text{C}$  and  $\delta^{18}\text{O}$  signatures in the Neoproterozoic carbonates of the Comba Basin, Republic of the Congo: implications for regional correlations and Marinoan deglaciation. *Precambrian Research*.
- Rodrigues, J.B., 2008. Proveni ncia dos sedimentos dos grupos Canastra, Ibia, Vazante e Bambui. Um estudo de zirc es detr ticos e idades modelo Sm-Nd. PhD thesis, Instituto de Geoci ncias da Universidade de Bras lia, Bras lia, 129 p.
- Santos, R.V., S. de Alvarenga, C.J., Dardenne, M.A., Sial, A.N. & Ferreira, V.P., 2000. Carbon and oxygen isotope profiles across Meso-Neoproterozoic limestones from central Brazil: Bambui and Parano  groups. *Precambrian Research* 104, 107-122.
- Santos, R.V., Souza de Alvarenga, C.J., Babinski, M., Ramos, M.L.S., Cukrov, N., Fonseca, M.A., Sial, A.N., Dardenne, M.A. & Noce, C.M., 2004. Carbon isotopes of Neoproterozoic sequences from Southern S o Francisco craton and Araua  Belt, Brazil: Paleographic implications. *Journal of South American Earth Sciences* 18, 27-39.
- Sikorski, J., 1958. Echelle stratigraphique provisoire des  tages C1-C2-C3 du syst me Schisto-Calcaire du Bas-Congo. CIMINGA, note n 15.
- Straathof, G.B., 2011. Neoproterozoic low latitude glaciations: an African perspective. Unpublished Ph.D. Thesis, University of Edinburgh, Scotland.
- Tack, L., Wingate, M.T.D., Li geois, J.-P., Fernandez-Alonso, M. & Beblond, A., 2001. Early Neoproterozoic magmatism (1000-910 Ma) of the Zadinian and Mayumbian Groups (Bas-Congo): onset of

- Rodinia rifting at the western edge of the Congo craton. *Precambrian Research* 110, 277-306.
- Tait, J., Delpomdor, F., Pr at, A., Tack., L., Straathof, G. & Kanda Nkula, V., 2011. Neoproterozoic sequences of the West Congo and Lindi/Ubangi Supergroups in the Congo Craton, Central Africa. In: Arnaud, E., Halverson, G.L. & Shields-Zhou, G., (eds), *The geological record of Neoproterozoic glaciations*. Geological Society, London, *Memoirs* 36, 185-194.
- Thi blemont, D., Castaing, C., Billa, M., Bouton, P. & Pr at, A., 2009. Notice explicative de la Carte g ologique et des Ressources min rales de la R publique gabonaise   1/1 000 000. Editions DGMG - Minist re des Mines, du P trole, des Hydrocarbures, Libreville, 381p.
- Trompette, R. & Boudzoumou, F., 1988. Paleogeographic significance of stromatolite buildups on late Proterozoic platform: the example of the West Congo basin. *Palaeogeography, Palaeoclimatology, Palaeoecology* 66, 101-112.
- Uhlein, G.J., de Carvalho, J.F.M.G., Uhlein, A., Caxito, F.A., Halverson, G.P. & Sial A.N., 2012. Estratigrafia e sedimentologia da Forma o Carrancas, Grupo Bambu , nas regi es de Belo Horizonte e Pitangui, MG. *Geonomos* 20 (2), 79-97.
- Warren, L.V., Quaglio, F., Riccomini, C., Simoes, M.G., Poir , D.G., Strikis, N.M., Anelli, A. & Strikis, P.C., 2014. The puzzle assembled: Ediacaran guide fossil *Claudina* reveals an old proto-Gondwana seaway. *Geology* 42 (5), 391-394.